Pergamon

J. Mech. Phys. Solids, Vol. 44, No. 11, pp. 1831–1866, 1996

0022-5096/96 $15.00+0.00

PII: S0022-5096(96)00056-7

DYNAMIC CRACK PROPAGATION IN PIEZOELECTRIC MATERIALS—PART II. VACUUM SOLUTION

SHAOFAN LI

Department of Mechanical Engineering, Northwestern University, Evanston, Illinois, U.S.A.

PETER A. MATAGA†

Software Production Research Department, Bell Laboratories, Naperville, Illinois, U.S.A.

(*Received* 13 *March* 1995; *in revised form* 19 *March* 1996)

ABSTRACT

In Part I of this work, antiplane dynamic crack propagation in piezoelectric materials was studied under the condition that crack surfaces behaved as though covered with a conducting electrode. Piezoelectric surface wave phenomena were clearly seen to be critical to the behavior of the moving crack. Closed form results were obtained for stress and electric displacement intensities at the crack tip in the subsonic crack speed range; the major result is that the energy release rate vanishes as the crack speed approaches the surface (Bleustein–Gulyaev) wave speed.

In this paper, an alternative assumption is made that between the growing crack surfaces there is a permeable vacuum free space, in which the electrostatic potential is nonzero. By coupling the piezoelectric equations of the solid phase with the electric charge equation in the vacuum region, a closed form solution is again obtained. In contrast to the electrode case of Part I, this case allows both applied charge and applied traction loading. In addition, the work of Part I is extended to examine piezoelectric crack propagation over the full velocity range of subsonic, transonic and supersonic speeds.

Several aspects of the results are explored. The energy release rate in this case does not go to zero when the crack propagating velocity approaches the surface wave speed, even if there is only applied traction loading. When the crack exceeds the Bleustein–Gulyaev wave speed, the character of the crack-tip singularities of the physical fields depends on both speed regime and type of loading. At the other extreme, the quasi-static limit of the dynamic solution furnishes a set of new static solutions. The general permeability assumptions made here allow for fully coupled conditions that are ruled out by the *a priori* interfacial assumptions made in previously published solutions. Copyright © 1996 Elsevier Science Ltd

Keywords: A. crack propagation and arrest, A. dynamic fracture, A. electromechanical process, B. piezoelectric material, C. piezoelectric effect.

1. INTRODUCTION

In a previous paper (Li and Mataga, 1996), subsequently referred to as "Part I", the problem of antiplane dynamic crack propagation in piezoelectric materials was formulated. The solution was obtained in closed form under the assumption that the crack surfaces behaved as though covered with a conducting electrode. Those results clearly show that piezoelectric surface wave phenomena are critical to the behavior

† Part of this work was carried out while the author was a member of the Department of Aerospace Engineering, Mechanics & Engineering Science, University of Florida, U.S.A.

of the moving crack; the reader is referred to Part I for a description of the relevance of the Bleustein–Gulyaev surface wave. Closed form results were obtained for stress and electric displacement intensities at the crack tip in the subcritical crack speed range; the major result is that the energy release rate vanishes as the crack speed approaches the Bleustein–Gulyaev wave speed.

The "electrode" case may serve as a good mathematical model for cases in which the void inside the growing crack is a stress-free, conducting included phase, but physically this is of limited applicability. Furthermore, the driving force studied in Part I is a distribution of crack face tractions only; there is no electric loading on the boundary. In this paper, we extend the previous results by relaxing these limitations. The crack included phase is modeled as a stress-free permeable vacuum space; this allows the external loadings along the boundary to include applied electric charge as well as applied tractions. In addition, the full crack extension speed range is investigated, whereas for the electrode case only the subcritical regime was analyzed.

One motivation of these extensions is to study how an induced electric field affects dynamic energy release rate under different electric boundary conditions, and, in particular, whether surface wave speed still appears to be the upper speed limit for crack propagation. For opening mode crack propagation in a purely elastic material, when the crack velocity approaches the Rayleigh wave speed, the energy release rate goes to zero, indicating that the Rayleigh wave speed serves as a speed barrier for propagating cracks.† Naturally, one would expect that the Bleustein–Gulyaev wave speed would also behave like a speed barrier for crack propagation in a piezoelectric medium. Indeed, for the case considered in Part I, under the electrode type of boundary condition, the total energy release rate does go to zero when crack speed approaches the Bleustein–Gulyaev wave speed, seemingly supporting this expectation. However, the fact that the boundary condition of a conductive crack surface forces a uniform distribution of electrostatic potential along the crack surfaces, which automatically eliminates the electrical contribution to dynamic energy release rate. Thus, further examination is necessary.

This question is intrinsically linked to a critical issue of piezoelectric fracture: the imposition of general electrical boundary conditions on the crack surfaces. The key question here is whether the void between the crack surfaces is permeable. In reality, as observed by Suo *et al.* (1992), there is a permeable free space inside the opening crack:

> "Specifically, for piezoelectric ceramics, the permittivity is 10^3 times higher than environment (e.g. air or silicone oil). A crack may be thought of as a low-capacitance medium carrying a potential drop."

Hitherto, the general problem has not been solved. In published static analyses, an impermeability approximation has typically been made in order to simplify the analysis. For example, Pak (1990, 1992) has argued that if the ratio of free space permittivity and material space permittivity $\varepsilon_f/\varepsilon_m$ is small, the crack may be approximated as an impermeable cavity. As Pak observes, the resulting interfacial condition decouples

† In reality, when the crack speed is up to about 70% of Rayleigh wave speed, crack bifurcation is predicted and observed (Yoffe, 1951).

the field equations for the domains occupied by the cavity and the surrounding piezoelectric material, allowing solution by consideration of the latter alone.

Despite the fact that this impermeability assumption is overwhelmingly favored in static analysis, uncertainty about its validity has been raised. To test the physical basis of the impermeability hypothesis, McMeeking (1989) calculated the electroelastic field in a 2-D isotropic dielectric body with an elliptical flaw. He found that the concentrations of both the mechanical and electrical field are controlled by a parameter

$$\frac{\varepsilon_f}{\varepsilon_m}\frac{b}{a}, \tag{1}$$

where a/b is the aspect ratio of the ellipse. He concluded that:

> "The impermeable crack solution serves as a good approximation to actual solutions, ..., as long as $\varepsilon_f/\varepsilon_m$ is less than one tenth of b/a and $b/a \ll 1$. Thus, the flaw must exceed a certain degree of bluntness dependent on the ratio of permittivities. When b/a is comparable to $\varepsilon_f/\varepsilon_m$, there is a field concentration, but the behavior cannot be approximated by the impermeable crack.... Thus, the question of whether the slender flaw can be treated as an impermeable crack must be decided on a case-by-case basis."

In this paper, we are able to pursue physical generality without losing the mathematical advantages of the antiplane problem. We discard the impermeability approximation and study the propagating crack containing a permeable vacuum environment, solving the coupled wave equations in both the cracked piezoelectric region and the interior vacuum region between the crack surfaces.

There are a number of intriguing consequences of this more general boundary condition. First, a potential distribution may now exist along the crack surfaces, leading to the possibility of a potential drop across the crack. This results in a Bleustein–Gulyaev wave of different character from that arising in the electrode case of Part I. Somewhat unexpectedly, even under purely traction loading, the energy release rate of the vacuum solution does not go to zero as crack speed approaches the Bleustein–Gulyaev wave speed c_{bg}. This is quite different from the parallel elastodynamic (in-plane) case, and from the "electrode" solution obtained in Part I. Moreover, applied electric charge loading may affect the energy release rate by decreasing it, implying that this type of external loading can retard crack extension.

Second, particularly because the surface wave speed may not provide a barrier to crack propagation for this general case, we have studied crack propagation over the full speed range: sub-Bleustein–Gulyaev speed ($v < c_{bg}$), transonic speed ($c_{bg} < v < c$), and supersonic speed ($v > c$). The results show a variety of asymptotic behavior with change in crack speed regime. For the crack driven by mechanical load alone, there is no singularity in mechanical or electrical near-tip fields after crack extension speed exceeds the Bleustein–Gulyaev wave speed. In contrast to the purely elastic case, however, there are nonzero fields surviving in the piezoelectric body ahead of the crack tip, even when the crack is traveling at supersonic speed. On the other hand, if an electric charge loading is applied to the crack faces, the square root

singularity in physical fields is retained throughout the speed range, though the dynamic intensity factors change.

Third, at the other end of the speed range, the quasi-static ($v \to 0$) limit of the dynamic solution furnishes a set of new static solutions. The general permeability assumptions made here allow for fully coupled conditions that are ruled out by the *a priori* interfacial assumptions made in previously published solutions. An important consequence of this coupling is the existence of both self-induced and cross-over singular fields for each type of loadings.

2. STATEMENT OF THE PROBLEM

For the sake of a self-contained presentation (a more detailed presentation may be found in Part I), the basic governing equations of piezoelectricity in the anti-plane mode are briefly reviewed here. The anti-plane dynamic problem in a hexagonal piezoelectric medium (*6mm*) can be described by the following equations (Bleustein, 1968).

$$c_{44}^{E}\nabla^2 w + e_{15}\nabla^2\phi = \rho\ddot{w}, \tag{2}$$

$$e_{15}\nabla^2 w - \varepsilon_{11}^{S}\nabla^2\phi = 0. \tag{3}$$

Here w is the antiplane displacement (the Z-axis is assumed to be aligned with the hexagonal symmetry axis), ϕ is the electric potential, and ρ is the mass density. ∇^2 is the in-plane (X, Y) Laplacian, and a dot denotes material time derivative. The coefficients are the appropriate components of the elastic, dielectric and piezoelectric stress constant tensors.

Through the transformation

$$\psi \triangleq \phi - \frac{e_{15}}{\varepsilon_{11}} w, \tag{4}$$

the governing equations can be decoupled as

$$\begin{cases} \nabla^2 w = \dfrac{\rho}{\bar{c}_{44}}\ddot{w}, \\ \nabla^2\psi = 0, \end{cases} \tag{5}$$

where

$$\bar{c}_{44} \triangleq c_{44}^{E} + \frac{e_{15}^2}{\varepsilon_{11}^{S}} \tag{6}$$

is the piezoelectrically stiffened elastic constant.

In terms of independent variables w and ψ, the constitutive equations can then be written as

$$\sigma_{XZ} = \bar{c}_{44}\frac{\partial w}{\partial X} + e_{15}\frac{\partial\psi}{\partial X}, \tag{7}$$

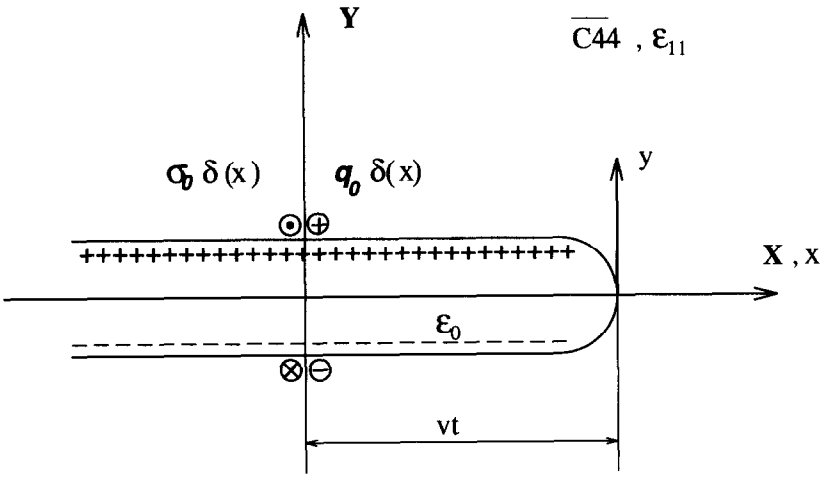

Fig. 1. Running crack abutted to permeable vacuum at the crack interface.

$$\sigma_{YZ} = \bar{c}_{44}\frac{\partial w}{\partial Y} + e_{15}\frac{\partial \psi}{\partial Y}, \tag{8}$$

$$D_X = -\varepsilon_{11}\frac{\partial \psi}{\partial X}, \tag{9}$$

$$D_Y = -\varepsilon_{11}\frac{\partial \psi}{\partial Y}. \tag{10}$$

As in Part I, we consider a semi-infinite crack in an unbounded piezoelectric body, assuming that the crack is initially at rest starts to propagate at constant speed v after external loads are applied at $t = 0$. It is convenient to operate in the frame of a moving coordinate system, i.e.

$$x = X - vt, \quad y = Y, \quad z = Z. \tag{11}$$

In this paper, we envisage that there is a permeable medium of negligible mechanical influence inside the crack, occupying the region (Fig. 1)

$$\Omega_v(t) \triangleq \{(x, y) | -\infty < x < 0, \quad -\delta < y < \delta, \quad \delta \to 0\}. \tag{12}$$

Let Ω denote the whole x–y plane. The cracked piezoelectric body occupies the region $\Omega - \Omega_v$. Accordingly, the equations of motion in the piezoelectric medium and the Maxwell equation in the vacuum strip are

$$\begin{cases} s^2\dfrac{\partial^2 w}{\partial x^2} + \dfrac{\partial^2 w}{\partial y^2} + \dfrac{2v}{c^2}\dfrac{\partial^2 w}{\partial x \partial t} - \dfrac{1}{c^2}\dfrac{\partial^2 w}{\partial t^2} = 0 & \text{in } \Omega - \Omega_v, \quad \text{(a)} \\ \dfrac{\partial^2 \psi}{\partial x^2} + \dfrac{\partial^2 \psi}{\partial y^2} = 0 & \text{in } \Omega - \Omega_v, \quad \text{(b)} \\ \dfrac{\partial^2 \tilde{\phi}}{\partial x^2} + \dfrac{\partial^2 \tilde{\phi}}{\partial y^2} = 0 & \text{in } \Omega_v, \quad \text{(c)} \end{cases} \tag{13}$$

where

$$s \triangleq \left(1 - \frac{v^2}{c^2}\right)^{1/2} \tag{14}$$

and

$$c \triangleq \left(\frac{\bar{c}_{44}}{\rho}\right)^{1/2} \tag{15}$$

is the bulk shear horizontal (SH) wave speed in the piezoelectrical material.

For the case considered in this paper, the applied loadings may be electrical as well as mechanical. We consider a kernel problem in which a line load pair and line charge pair are suddenly applied at the origin at $t = 0$ (Fig. 1). The mechanical boundary conditions are similar to those discussed in Part I. Because of the antisymmetry of the problem (including the electric loading), we consider the upper half plane only and apply

$$\begin{cases} \sigma_{xz}(x, 0^+, t) = -\delta(x+vt)H(t) & x < 0, \\ w(x, 0^+, t) = 0 & x > 0. \end{cases} \tag{16}$$

It will later be convenient to put the conditions into expanded form by introducing two new functions $\sigma_+(x, t)$ and $w_-(x, t)$, such that

$$\sigma_+(x, t) \triangleq \begin{cases} 0 & x < 0, \\ \sigma_{yz}(x, 0^+, t) & x > 0, \end{cases} \tag{17}$$

$$w_-(x, t) \triangleq \begin{cases} w(x, 0^+, t) & x < 0, \\ 0 & x > 0, \end{cases} \tag{18}$$

so that

$$\begin{cases} \sigma_{yz}(x, 0^+, t) = -P_0\delta(x+vt)H(t) + \sigma_+(x, t) & -\infty < x < \infty, \\ w(x, 0^+, t) = w_-(x, t) + 0 & -\infty < x < \infty. \end{cases} \tag{19}$$

The electrical parts of the boundary conditions are imposed in the standard form of electrostatics (e.g. Jackson, 1974). At an interface between two dissimilar dielectric materials, the boundary conditions are as follows

$$\begin{cases} \mathbf{n} \cdot (\mathbf{D}^{(2)} - \mathbf{D}^{(1)}) = q_0, \\ \mathbf{n} \times (\mathbf{E}^{(2)} - \mathbf{E}^{(1)}) = 0, \end{cases} \tag{20}$$

where q_0 is the interfacial trapped charge density.

When the density of electric charge in the interface is zero, the interfacial conditions may be taken as

$$\begin{cases} \mathbf{n} \cdot (\mathbf{D}^{(2)} - \mathbf{D}^{(1)}) = 0, \\ \phi^{(2)} - \phi^{(1)} = 0, \end{cases} \tag{21}$$

for this particular configuration (Pak, 1990).

Again, by the argument of superposition onto an initially quiescent solution, and by the decay of local electrostatic disturbances, we assume that in the perturbed field at $|y| \to \infty$

$$\sigma_{yz}(x, y, t) = 0 \quad \text{and} \quad D_y(x, y, t) = 0. \tag{22}$$

It should be noted that since $\tilde{\phi}(x, y, t)$ is limited to lying within a semi-infinite strip, it is not subjected the boundary condition at infinity.

3. CRACK PROPAGATION AT DIFFERENT EXTENSION SPEEDS

The first extension considered here is to restrict loading to the traction case considered in Part I, and examine the consequences of the modified crack surface conditions. The work of Part I is also extended by allowing crack extension speeds that exceed the piezoelectric surface wave speed. The primary concern is the asymptotic behavior of the electroelastic fields, rather than the full set of closed form solutions.

In the absence of charge loading on the crack faces, the boundary conditions for our problem may be written

$$\begin{cases} \sigma_{yz}(x, 0^+, t) = -P_0 \delta(x+vt)H(t) + \sigma_+(x, t) & -\infty < x < \infty, \quad \text{(a)} \\ w(x, 0^+, t) = w_-(x, t) + 0 & -\infty < x < \infty, \quad \text{(b)} \end{cases} \tag{23}$$

and

$$\begin{cases} D_y(x, 0^+, t) - \tilde{D}_y(x, 0^+, t) = 0 & -\infty < x < 0, \quad \text{(a)} \\ \psi(x, 0^+, t) + \dfrac{e_{15}}{\varepsilon_{11}} w(x, 0^+, t) = \tilde{\phi}(x, 0^+, t) & -\infty < x < 0. \quad \text{(b)} \end{cases} \tag{24}$$

As will be shown later, the solution of this problem is the essential part of the general case.

Applying multiple Laplace transforms to [13(a)–(c)], to convert them into a set of ordinary differential equations,

$$\left[\frac{\mathrm{d}^2}{\mathrm{d}y^2} - p^2\left(\frac{1}{c^2} - 2\frac{v}{c^2}\zeta - s^2\zeta^2\right)\right]\hat{w}^*(\zeta, y, p) = 0 \quad \forall(\zeta, y, p) \in \Omega_p - \Omega_{pv}, \tag{25}$$

$$\left[\frac{\mathrm{d}^2}{\mathrm{d}y^2} - p^2(\varepsilon^2 - \zeta^2)\right]\hat{\psi}^*(\zeta, y, p) = 0 \quad \forall(\zeta, y, p) \in \Omega_p - \Omega_{pv}, \tag{26}$$

$$\left[\frac{\mathrm{d}^2}{\mathrm{d}y^2} - p^2(\varepsilon^2 - \zeta^2)\right]\hat{\tilde{\phi}}^*(\zeta, y, p) = 0 \quad \forall(\zeta, y, p) \in \Omega_{pv}, \tag{27}$$

where $\varepsilon \to 0^+$ (see Part I for a more detailed discussion of this use of an auxiliary perturbation parameter) and

$$\Omega_p \triangleq \mathbf{C}(\zeta) \times \mathbf{R}(y) \times \mathbf{C}(p), \tag{28}$$

$$\Omega_{vp} \triangleq \mathbf{C}(\zeta) \times [-\delta, \delta] \times \mathbf{C}(p). \tag{29}$$

Consideration of the boundary conditions at infinity leads to solutions of the form

$$\hat{w}^*(\zeta, y, p) = \operatorname{sgn}(y) \frac{1}{p^2} A(\zeta) \exp(-p\alpha|y|), \tag{30}$$

$$\hat{\psi}^*(\zeta, y, p) = \operatorname{sgn}(y) \frac{1}{p^2} B(\zeta) \exp(-p\beta|y|), \tag{31}$$

$$\hat{\tilde{\phi}}^*(\zeta, y, p) = \operatorname{sgn}(y) \frac{1}{p^2} C(\zeta) \exp(p\beta|y|), \tag{32}$$

where

$$\alpha(\zeta) \triangleq \sqrt{\frac{1}{c^2} - \frac{2v\zeta}{c^2} - s^2\zeta^2} = \mathrm{s}\sqrt{\left(\zeta + \frac{1}{c-v}\right)\left(\frac{1}{c+v} - \zeta\right)}, \tag{33}$$

$$\beta(\zeta) \triangleq \lim_{\varepsilon \to 0} \sqrt{\varepsilon^2 - \zeta^2} \tag{34}$$

were introduced in Part I.

Remark 1. The choice of solution in (32) does not come from the boundary condition at infinity, since $\tilde{\phi}(x, y, t)$ is not subjected to any boundary conditions at $|y| \to \infty$. The complete form of the solution should be

$$\hat{\tilde{\phi}}^*(\zeta, y, p) = \frac{\operatorname{sgn}(y)}{p^2} (C_+(\zeta) \exp(p\beta|y|) + C_-(\zeta) \exp(-p\beta|y|)). \tag{35}$$

The choice in (32), however, renders a physically plausible result. Specifically, (32) predicts the surface wave solution.

The transformed version of (24a) and (24b) provide the relationship between unknown functions $A(\zeta)$, $B(\zeta)$ and $C(\zeta)$

$$\frac{e_{15}}{\varepsilon_{11}} A(\zeta) + B(\zeta) = C(\zeta), \tag{36}$$

$$\varepsilon_{11}\beta(\zeta)B(\zeta) + \varepsilon_0\beta(\zeta)C(\zeta) = 0. \tag{37}$$

These can be solved simultaneously together with (23b) to obtain

$$A(\zeta) = U_-(\zeta), \tag{38}$$

$$B(\zeta) = -\frac{e_{15}}{\varepsilon_{11}} \frac{\varepsilon_0}{\varepsilon_{11} + \varepsilon_0} U_-(\zeta), \tag{39}$$

$$C(\zeta) = \frac{e_{15}}{\varepsilon_{11} + \varepsilon_0} U_-(\zeta), \tag{40}$$

where

$$U_-(\zeta) \triangleq p\int_{-\infty}^{0} w^*(x,0^+,t)\exp(-p\zeta x)\,\mathrm{d}x$$

$$= p\int_{-\infty}^{0} w_-^*(x,t)\exp(-p\zeta x)\,\mathrm{d}x. \tag{41}$$

Due to symmetry, it is sufficient to only consider the solution for $y \geqslant 0$. The stresses and electric displacements can then be expressed in terms of the single unknown function $U_-(\zeta)$

$$\sigma_{xz}^*(x,y,p) = \frac{\bar{c}_{44}}{2\pi\mathrm{i}}\left(\int_{\zeta_\alpha-\mathrm{i}\infty}^{\zeta_\alpha+\mathrm{i}\infty} \zeta U_-(\zeta)\exp\left[-p(\alpha y-\zeta x)\right]\mathrm{d}\zeta\right.$$

$$\left.-k_v^2\int_{\zeta_\beta-\mathrm{i}\infty}^{\zeta_\beta+\mathrm{i}\infty} \zeta U_-(\zeta)\exp\left[-p(\beta y-\zeta x)\right]\mathrm{d}\zeta\right), \tag{42}$$

$$\sigma_{yz}^*(x,y,p) = -\frac{\bar{c}_{44}}{2\pi\mathrm{i}}\left(\int_{\zeta_\alpha-\mathrm{i}\infty}^{\zeta_\alpha+\mathrm{i}\infty} \alpha(\zeta)U_-(\zeta)\exp[-p(\alpha y-\zeta x)]\,\mathrm{d}\zeta\right.$$

$$\left.-k_v^2\int_{\zeta_\beta-\mathrm{i}\infty}^{\zeta_\beta+\mathrm{i}\infty} \beta(\zeta)U_-(\zeta)\exp\left[-p(\beta y-\zeta x)\right]\mathrm{d}\zeta\right), \tag{43}$$

$$D_x^*(x,y,p) = -\frac{e_{15}}{2\pi\mathrm{i}}\int_{\zeta_\beta-\mathrm{i}\infty}^{\zeta_\beta+\mathrm{i}\infty} \zeta U_-(\zeta)\exp\left[-p(\beta y-\zeta x)\right]\mathrm{d}\zeta, \tag{44}$$

$$D_y^*(x,y,p) = \frac{e_{15}}{2\pi\mathrm{i}}\int_{\zeta_\beta-\mathrm{i}\infty}^{\zeta_\beta+\mathrm{i}\infty} \beta(\zeta)U_-(\zeta)\exp\left[-p(\beta y-\zeta x)\right]\mathrm{d}\zeta, \tag{45}$$

where

$$-\frac{1}{c-v} < \zeta_\alpha < \frac{1}{c+v}, \quad -\varepsilon < \zeta_\beta < \varepsilon, \tag{46}$$

and

$$k_v^2 \triangleq \frac{e_{15}^2}{\varepsilon_{11}c_{44}}\frac{\varepsilon_0}{\varepsilon_{11}+\varepsilon_0}. \tag{47}$$

Substituting (43) into the transformed stress boundary condition (23a), we obtain the following Wiener–Hopf equation

$$\Sigma_+(\zeta) + \frac{P_0}{v(\zeta-1/v)} = K(\zeta)U_-(\zeta), \tag{48}$$

where

$$K(\zeta) = -c_{44}[\alpha(\zeta)-k_v^2\beta(\zeta)], \tag{49}$$

Table 1. *Electroacoustic constants of several piezoelectric materials*

Compound	$k_e \equiv \sqrt{\frac{e_{15}^2}{c_{44}\varepsilon_{11}^S}}$	$k_v \equiv k_e\sqrt{\frac{\varepsilon_0}{\varepsilon_0+\varepsilon_{11}}}$	ε_{11}^S $(10^{-9}F/m)$	$r \triangleq \varepsilon_0/\varepsilon_{11}$
PZT-4[a]	0.7026	0.0260	6.4634	0.0014
PZT-5[a]	0.6850	0.0226	8.1103	0.0011
$BaTiO_3$[a]	0.4799	0.0144	9.8722	8.986×10^{-4}
PZT 65/35[b]	0.4921	0.0197	5.660	0.0016
ZnO[c]	0.2586	0.0837	0.0757	0.1170

[a] Berlincourt *et al.*, 1964
[b] Chen, 1983
[c] Auld, 1973

$$\Sigma_+(\zeta) \triangleq p\int_0^{+\infty} \sigma_+^*(x,p)\exp(-p\zeta x)\,dx$$
$$= p\int_0^{+\infty} \sigma_{yz}^*(x,0^+,p)\exp(-p\zeta x)\,dx. \tag{50}$$

The Wiener–Hopf equation (48) has identical structure to that solved in Part I, except that the new Bleustein–Gulyaev function has a different electromechanical coupling coefficient k_v, i.e.

$$BG(\zeta) = \alpha(\zeta) - k_v^2\beta(\zeta). \tag{51}$$

This function corresponds to a second kind of Bleustein–Gulyaev piezoelectric surface wave (the first being that corresponding to a half space with electrode boundary, as considered in Part I). This "vacuum abutted" surface wave (Bleustein, 1968; Ikeda, 1990) propagates at speed c_{bg} defined by†

$$c_{bg} \triangleq \left(\frac{\bar{c}_{44}}{\rho}\right)^{1/2}\sqrt{1-k_v^4}. \tag{52}$$

It should be noted that there is typically a huge difference between the electromechanical coupling coefficient k_e and k_v. For a quantitative comparison, see Table 1.

Since crack speed affects both number and location of roots of the Bleustein–Gulyaev wave function $BG(\zeta)$, the product factorization necessary to solve the Wiener–Hopf equation (48) is different for each crack speed regime. Here we consider three regimes: subcritical ($v < c_{bg}$), transonic ($c_{bg} < v < c$) and supersonic ($v > c$).

† To distinguish the two different BG wave velocities, we denote the BG wave with electrode boundary condition as $c_{bg}^{(e)}$ and the BG wave with vacuum boundary condition as $c_{bg}^{(v)}$. In this paper, unless otherwise specified, the velocity c_{bg} is always understood as $c_{bg}^{(v)}$.

3.1. *Subcritical case* $v < c_{bg}$

The case for which $v < c_{bg}$ has been discussed in Part I under a different BG wave speed. There are two distinct real roots of the BG wave function

$$\zeta_1 = -\frac{1}{c_{bg}-v}, \quad \zeta_2 = \frac{1}{c_{bg}+v}. \tag{53}$$

Each of them lies in a different half ζ-plane, $\zeta_1 \in P_-(\zeta)$ and $\zeta_2 \in P_+(\zeta)$, where

$$P_-(\zeta) \triangleq \{\zeta \in \mathbf{C} | \mathrm{Re}(\zeta) < \varepsilon\}, \tag{54}$$

$$P_+(\zeta) \triangleq \{\zeta \in \mathbf{C} | \mathrm{Re}(\zeta) > -\varepsilon\}. \tag{55}$$

As shown in Part I, the result of product factorization gives

$$BG(\zeta) = (s-k_v^2)\sqrt{[1/(c_{bg}+v)-\zeta][1/(c_{bg}-v)+\zeta]}S_+(\zeta)S_-(\zeta), \tag{56}$$

where

$$S_+(\zeta) = \sqrt{\frac{(1/(c_{bg}-v)+\zeta)}{(1/(c_{bg}-v)+\zeta)}}\exp\left\{-\frac{1}{\pi}\int_\varepsilon^{1/(c-v)} \arctan[\Theta(-\eta)]\frac{d\eta}{\eta+\zeta}\right\}, \tag{57}$$

$$S_-(\zeta) = \sqrt{\frac{(1/(c_{bg}+v)-\zeta)}{(1/(c+v)-\zeta)}}\exp\left\{-\frac{1}{\pi}\int_\varepsilon^{1/(c+v)} \arctan[\Theta(\eta)]\frac{d\eta}{\eta-\zeta}\right\}, \tag{58}$$

with

$$\Theta(\eta) \triangleq \frac{k_e^2\sqrt{\eta^2-\varepsilon^2}}{s\sqrt{(1/(c-v)+\eta)(1/(c+v)-\eta)}}. \tag{59}$$

The final solution of (48) is

$$\begin{cases} U_-(\zeta) = -\dfrac{P_0}{\sqrt{cv}}\dfrac{(s+k_e^2)}{c_{44}(\zeta-1/v)}\dfrac{c^2}{(c_{bg}+v)}\dfrac{\mathscr{D}_+(1/v)}{\sqrt{c-v}}\dfrac{\mathscr{D}_-(\zeta)}{\sqrt{(1-k_e^4)}}\dfrac{\sqrt{1/(c+v)-\zeta}}{(1/(c_{bg}+v)-\zeta)}, \\ \Sigma_+(\zeta) = \dfrac{P_0}{v(\zeta-1/v)}\left[\dfrac{D_+(1/v)}{D_+(\zeta)}\sqrt{\dfrac{v(c_{bg}-v)}{c_{bg}}}\sqrt{1/(c_{bg}-v)+\zeta}-1\right], \end{cases} \tag{60}$$

where

$$D_\pm(\zeta) = \frac{1}{S_\pm(\zeta)}, \tag{61}$$

$$\mathscr{D}_\pm(\zeta) = \exp\left\{\frac{1}{\pi}\int_\varepsilon^{1/(c\pm v)} \arctan[\Theta(\mp\eta)]\frac{d\eta}{\eta\pm\zeta}\right\}. \tag{62}$$

As $|\zeta| \to \infty$, one can show that

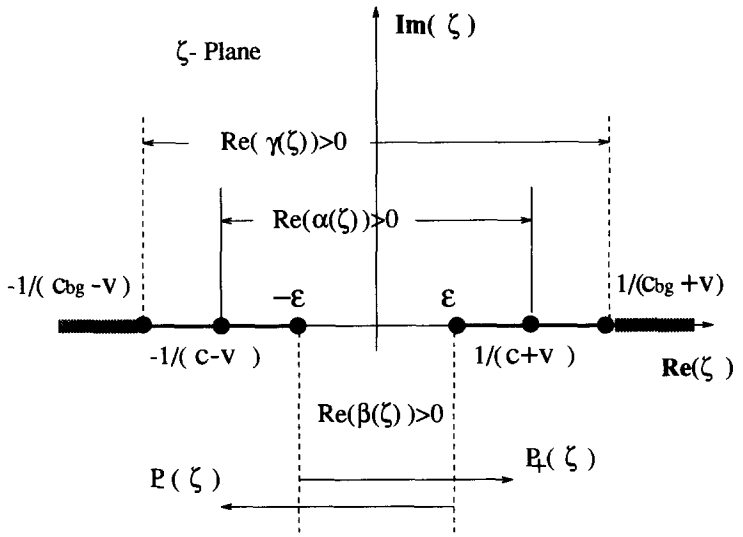

Fig. 2. Branch cuts and branch points of $S(\zeta)$ ($v < c_{bg}$).

$$U_-(\zeta) \to \mathcal{O}(\zeta^{-3/2}), \quad \Sigma_+(\zeta) \to \mathcal{O}(\zeta^{-1/2}). \tag{63}$$

Since, by the Abel theorem,

$$\lim_{x\to 0^+} (\pi x)^{1/2} \sigma_+^*(x,p) = \lim_{\zeta \to +\infty} (p\zeta)^{1/2} \frac{\Sigma_+(\zeta)}{p} \tag{64}$$

the stress field exhibits a square root singularity at the running crack tip. Manipulation of the results above allows the expression of the stress intensity factor of the fundamental solution as a function of crack extent and speed

$$K_{IIIT}^{(\sigma)}(vt, v) = \sqrt{\frac{2}{\pi}} P_0 \frac{(1 - v/c_{bg})}{\sqrt{1 - v/c}} \frac{\mathcal{D}_+(1/v)}{\sqrt{vt}}. \tag{65}$$

In the notation $K_{IIIT}^{(\sigma)}$, the superscript (σ) stands for stress intensity factor and the subscript $IIIT$ indicates an antiplane traction loading only. This distinction is necessary, since it will be shown later that under mixed type of external loading, there is a stress concentration induced by the electric charge distribution along the crack surface. We could (as in Part I) also extract the intensity factor for the square-root singular electric displacement field, $K_{IIIT}^{(D)}$.

3.2. *Transonic case* $c_{bg} < v < c$

When the crack moving speed is in a range between surface wave velocity and bulk SH wave velocity, the crack is in a transonic speed range (Brock, 1977). After crack speed reaches the surface wave speed, the stress field as well as the electric displacement field undergo drastic change, which is reflected by the fact that all the roots of the Bleustein–Gulyaev function reside on the right half ζ-plane, i.e. $\zeta_1, \zeta_2 \in P_+(\zeta)$

$$\zeta_1 = \frac{1}{v+c_{bg}}, \quad \zeta_2 = \frac{1}{v-c_{bg}}. \tag{66}$$

Hence, the product factorization will take a different route. Equation (49) may be rewritten in the form

$$\begin{aligned} K(\zeta) &= -c_{44}(\alpha(\zeta)-k_v^2\beta(\zeta)) \\ &= c_{44}\gamma(\zeta)(\mathrm{i}(s-k_v^2))S^{(\mathrm{I})}(\zeta), \end{aligned} \tag{67}$$

where

$$S^{(\mathrm{I})}(\zeta) = \frac{\mathrm{i}(\alpha(\zeta)-k_v^2\beta(\zeta))}{(s-k_v^2)\gamma(\zeta)} \tag{68}$$

and

$$\gamma(\zeta) \triangleq \sqrt{[1/(v-c_{bg})-\zeta][1/(v+c_{bg})-\zeta]}. \tag{69}$$

Before the product decomposition

$$S^{(I)}(\zeta) = S_+^{(I)}(\zeta)S_-^{(I)}(\zeta) \tag{70}$$

is carried out, it is advantageous to find the change in argument of the complex function $S^{(I)}(\zeta)$ along the branch cut. From Fig. 3, one can find that in the upper half plane $P_-(\zeta)$

$$\Theta(\zeta) = \begin{cases} \arctan[\Xi^{(I)}(\zeta)]; & -1/(c-v) < \mathrm{Re}(\zeta) < -\varepsilon, \\ 0; & -\infty < \mathrm{Re}(\zeta) < -1/(c-v), \end{cases} \tag{71}$$

where

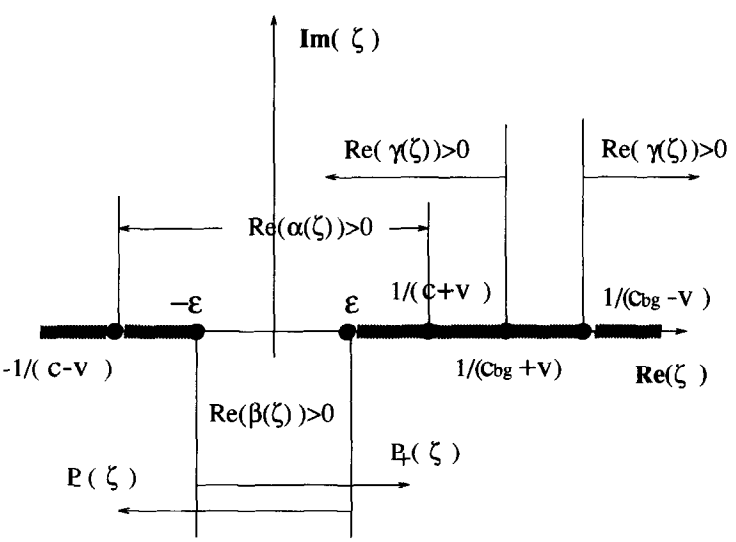

Fig. 3. Branch cuts and branch points of $S^{(I)}(\zeta)$ ($c_{bg} < v < c$).

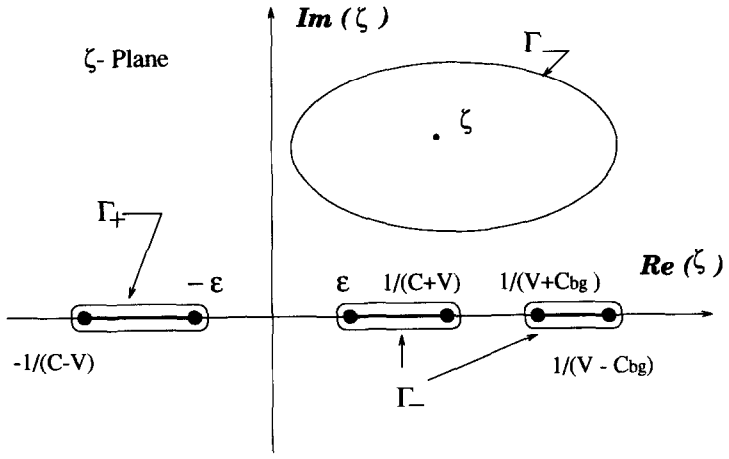

Fig. 4. Integration contours used for product decomposition of $S^{(t)}(\zeta)(c_{bg} < v < c)$.

$$\Xi^{(t)}(\zeta) \triangleq \frac{s\sqrt{(1/(c-v)+\zeta)}\sqrt{(1/(c+v)-\zeta)}}{k_v^2\sqrt{\zeta^2-\varepsilon^2}}. \tag{72}$$

Likewise, along the branch cut in upper half $P_+(\zeta)$ plane

$$\Theta(\zeta) = \begin{cases} \arctan[\Xi^{(t)}(\zeta)]; & \varepsilon < \mathrm{Re}(\zeta) < 1/(c+v), \\ 0; & 1/(c+v) < \mathrm{Re}(\zeta) < 1/(c_{bg}+v), \\ -\dfrac{\pi}{2}; & 1/(c_{bg}+v) < \mathrm{Re}(\zeta) < 1/(v-c_{bg}), \\ 0; & 1/(v-c_{bg}) < \mathrm{Re}(\zeta) < +\infty. \end{cases} \tag{73}$$

Based on this information, the inversion contours may be chosen as shown in Fig. 4.

The final product decomposition results in

$$S_+^{(t)}(\zeta) = \exp\left\{\frac{1}{\pi}\int_{\varepsilon}^{1/(c-v)} \arctan\left[\frac{s\sqrt{(1/(c-v)-\eta)}\sqrt{(1/(c+v)+\eta)}}{k_v^2\eta}\right]\frac{d\eta}{\eta+\zeta}\right\} \tag{74}$$

and

$$S_-^{(t)}(\zeta) = \sqrt{\frac{[1/(v-c_{bg})-\zeta]}{[1/(v+c_{bg})-\zeta]}}\,\mathscr{S}_-^{(t)}(\zeta), \tag{75}$$

where

$$\mathscr{S}_-^{(t)}(\zeta) = \exp\left\{\frac{1}{\pi}\int_{\varepsilon}^{1/(c+v)} \arctan\left[\frac{s\sqrt{(1/c-v)+\eta)}\sqrt{(1/(c+v)-\eta)}}{k_v^2\eta}\right]\frac{d\eta}{\eta-\zeta}\right\}. \tag{76}$$

By utilizing the product factorization results and following through the additive decomposition procedure, the Wiener–Hopf equation can be rearranged

$$ic_{44}(s-k_v^2)[1/(v-c_{bg})-\zeta]\mathscr{S}_-^{(t)}(\zeta)U_-(\zeta)-\frac{P_0}{v(\zeta-1/v)S_+^{(t)}(1/v)}$$
$$=\frac{P_0}{v(\zeta-1/v)}\left(\frac{1}{S_+^{(t)}(\zeta)}-\frac{1}{S_+^{(t)}(1/v)}\right)+\frac{\Sigma_+(\zeta)}{S_+^{(t)}(\zeta)}. \quad (77)$$

It is not difficult to show that as $\zeta \to \infty$

$$\left|ic_{44}(s-k_v^2)[1/(v-c_{bg})-\zeta]\mathscr{S}_-^{(t)}(\zeta)U_-(\zeta)-\frac{P_0}{v(\zeta-1/v)S_+^{(t)}(1/v)}\right| \sim \mathcal{O}(|\zeta|^{-1/2}).$$

Then the entire function to which both sides of the Wiener–Hopf equation (77) must be equal can only be the constant zero, which immediately leads to

$$\begin{cases} \Sigma_+(\zeta)=\dfrac{P_0}{v(\zeta-1/v)}\left(\dfrac{S_+^{(t)}(\zeta)}{S_+^{(t)}(1/v)}-1\right), & \text{(a)} \\ U_-(\zeta)=-\dfrac{iP_0}{c_{44}(s-k_v^2)}\dfrac{D_+^{t}(1/v)}{v(\zeta-1/v)}\dfrac{\mathscr{D}_-^{t}(\zeta)}{(1/(v-c_{bg})-\zeta)}, & \text{(b)} \end{cases} \quad (78)$$

where

$$D_+^{(t)}(1/v)=\frac{1}{S_+^{(t)}(1/v)}, \quad \mathscr{D}_-^{(t)}(\zeta)=\frac{1}{\mathscr{S}_-^{(t)}(\zeta)}. \quad (79)$$

Clearly, as $\zeta \to \infty$

$$\Sigma_+(\zeta) \to \mathcal{O}(\zeta^{-1}), \quad U_-(\zeta) \to \mathcal{O}(\zeta^{-2}), \quad (80)$$

which implies that all singular fields disappear. In particular

$$\lim_{x\to 0^+}(\pi x)^{1/2}\sigma_+^*(x,p)=\lim_{\zeta\to+\infty}(p\zeta)^{1/2}(\Sigma_+(\zeta)/p)$$
$$=\lim_{\zeta\to+\infty}\frac{P_0}{v}\frac{1}{\sqrt{p\zeta}}\left(\frac{S_+^{(t)}(\zeta)}{S_+^{(t)}(1/v)}-1\right)=0. \quad (81)$$

3.3. *Supersonic case* v > c

In a purely elastic medium, crack face tractions cannot drive a crack to propagate at supersonic speed (above the bulk shear wave speed in this case) unless there is a load acting at the crack tip, moving at supersonic speed to force the crack to move with it. In this case, the crack advances without warning, because the shear wave front is always behind the running crack tip [see Aki and Richards (1980), Freund (1990) for details].

Intuitively, some changes might be expected if the antiplane crack is travelling in a piezoelectric medium, since one of the governing equations—the electric charge equation—is elliptic, in fact being derived from a wave equation with its wave speed taken as infinity, as we have remarked in Part I. This means that field propagation is not limited to sonic velocities, as will be seen.

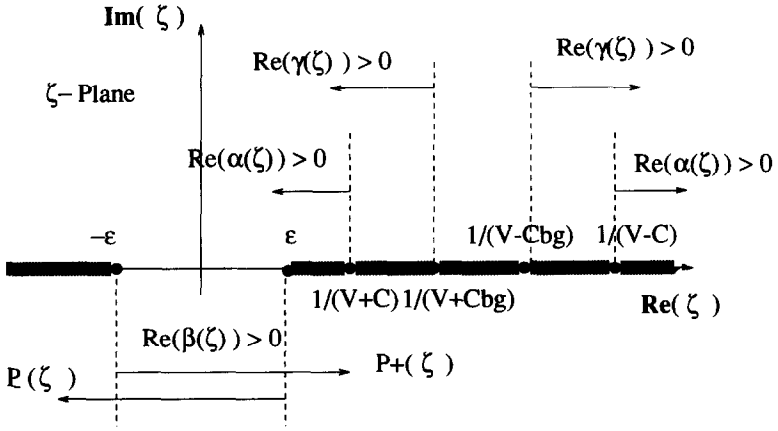

Fig. 5. Branch cuts and branch points of $S^{(s)}(\zeta)$ $(v > c)$.

For $v > c$, in place of s, a parameter

$$\kappa = \sqrt{\frac{v^2}{c^2} - 1} \tag{82}$$

is introduced, so that $\alpha(\zeta)$ can be rewritten as

$$\alpha(\zeta) \triangleq \sqrt{\kappa^2\zeta^2 - \frac{2v\zeta}{c^2} + \frac{1}{c^2}} = \sqrt{(1/(v-c)-\zeta)(1/(v+c)+\zeta)}. \tag{83}$$

The product decomposition for this case is of quite different character from those considered in the preceding sections. The branch cuts and the distribution of the branch points necessitate a different approach. Comparing Fig. 5 with Figs 2 and 3, note in particular the absence of any finite integration contours available to evaluate sectionally analytic functions. To construct an appropriate product decomposition, the inversion integral has to be evaluated along the whole branch cut in both $P_-(\zeta)$ and $P_+(\zeta)$ plane.

Let

$$\begin{aligned} BG(\zeta) &= \alpha(\zeta) - k_v^2\beta(\zeta) \\ &= \gamma(\zeta)(\kappa - \mathrm{i}k_v^2)S^{(s)}(\zeta), \end{aligned} \tag{84}$$

where

$$S^{(s)}(\zeta) = \frac{(\alpha(\zeta) - k_v^2\beta(\zeta))}{((\kappa - \mathrm{i}k_v^2)\gamma(\zeta))}. \tag{85}$$

The argument of $S^{(s)}(\zeta)$ along the branch cut in the upper half space $P_-(\zeta)$ is

$$\Theta(\zeta) = \arctan\left[\Xi^{(s)}(\zeta)\right]; \quad -\infty < \mathrm{Re}(\zeta) < -\varepsilon, \tag{86}$$

where

$$\Xi^{(s)}(\zeta) \triangleq \frac{(\kappa k_v^2)(\sqrt{(1/(v-c)-\zeta)(1/(c+v)-\zeta)}-\sqrt{\zeta^2-\varepsilon^2})}{\kappa^2\sqrt{(1/(v-c)-\zeta)(1/(c+v)-\zeta)}+k_v^4\sqrt{\zeta^2-\varepsilon^2}} \tag{87}$$

and arg $S^{(s)}(\zeta)$ along the branch cut in the upper half space $P_+(\zeta)$ is given by

$$\Theta(\zeta) = \begin{cases} \arctan[\Xi^{(s)}(\zeta)]; & \varepsilon < \mathrm{Re}(\zeta) < 1/(c+v), \\ -\arctan\left[\dfrac{\kappa}{k_v^2}\right]; & 1/(v+c) < \mathrm{Re}(\zeta) < 1/(v+c_{bg}), \\ -\arctan\left[\dfrac{k_v^2}{\kappa}\right]; & 1/(v+c_{bg}) < \mathrm{Re}(\zeta) < 1/(v-c_{bg}), \\ -\arctan\left[\dfrac{\kappa}{k_v^2}\right]; & 1/(v-c_{bg}) < \mathrm{Re}(\zeta) < 1/(v-c), \\ \arctan[\Xi^{(s)}(\zeta)]; & 1/(v-c) < \mathrm{Re}(\zeta) < \infty. \end{cases} \tag{88}$$

The corresponding decomposition is

$$S_+^{(s)}(\zeta) = \exp\left\{-\frac{1}{\pi}\int_\varepsilon^\infty \arctan[\Xi^{(s)}(-\eta)]\frac{d\eta}{\eta+\zeta}\right\}, \tag{89}$$

$$S_-^{(s)}(\zeta) = \left[\frac{(1/(v+c_{bg})-\zeta)(1/(v-c)-\zeta)}{(1/(v+c)-\zeta)(1/(v-c_{bg})-\zeta)}\right]^{k_1}\left[\frac{1/(v-c_{bg})-\zeta}{1/(v+c_{bg})-\zeta}\right]^{1/2-k_1}\mathscr{S}_-^{(s)}(\zeta), \tag{90}$$

where

$$\mathscr{S}_-^{(s)}(\zeta) \triangleq \exp\left\{-\frac{1}{\pi}\left(\int_\varepsilon^{1/(c+v)}\arctan[\Xi^{(s)}(\eta)]\frac{d\eta}{\eta-\zeta}+\int_{1/(v-c)}^\infty \arctan[\Xi^{(s)}(\eta)]\frac{d\eta}{\eta-\zeta}\right)\right\} \tag{91}$$

and

$$k_1(v,k_v) \triangleq \frac{1}{\pi}\arctan\frac{\kappa}{k_v^2}. \tag{92}$$

The Wiener–Hopf equation can now be rearranged as

$$\frac{\Sigma_+(\zeta)}{S_+^{(s)}(\zeta)}+\frac{P_0}{v(\zeta-1/v)}\frac{1}{S_+^{(s)}(\zeta)} = -c_{44}(\kappa-ik_v^2)\left(\frac{1/(v-c)-\zeta}{1/(v+c)-\zeta}\right)^{k_1}\frac{(1/(v-c_{bg})-\zeta)^{2k_1-1}}{(1/(v+c_{bg})-\zeta)^{2k_1}}\mathscr{S}_-^{(s)}(\zeta)U_-(\zeta). \tag{93}$$

Additive decomposition further separates sectionally analytic functions to their own analytic plane

$$\frac{\Sigma_+(\zeta)}{S_+^{(s)}(\zeta)}+\frac{P_0}{v(\zeta-1/v)}\left(\frac{1}{S_+^{(s)}(\zeta)}-\frac{1}{S_+^{(s)}(1/v)}\right) = -\frac{P_0}{v(\zeta-1/v)}\left(\frac{1}{S_+^{(s)}(1/v)}\right) - c_{44}(\kappa-ik_v^2)\left(\frac{1/(v-c)-\zeta}{1/(v+c)-\zeta}\right)^{k_1}\frac{(1/(v-c_{bg})-\zeta)^{2k_1-1}}{(1/(v+c_{bg})-\zeta)^{2k_1}}\mathscr{S}_-^{(s)}(\zeta)U_-(\zeta). \tag{94}$$

Consideration of asymptotic behavior and the requirement of an integrable energy density, followed by an application of the extended Liouville's theorem offers the final solutions

$$\begin{cases} \Sigma_+(\zeta) = \dfrac{P_0}{v(\zeta-1/v)}\left(\dfrac{S_+^{(s)}(\zeta)}{S_+^{(s)}(1/v)}-1\right), \\ U_-(\zeta) = -\dfrac{P_0\mathscr{D}_-^{(s)}(\zeta)}{v(\zeta-1/v)}\dfrac{D_+^{(s)}(1/v)}{c_{44}(\kappa-ik_v^2)}\left(\dfrac{1/(v+c)-\zeta}{1/(v-c)-\zeta}\right)^{k_1}\dfrac{(1/(v-c_{bg})-\zeta)^{2k_1-1}}{(1/(v+c_{bg})-\zeta)^{2k_1}}. \end{cases} \tag{95}$$

The asymptotic behavior of the above as $|\zeta| \to \infty$ makes it clear that no singular fields exist, just as in the transonic case, since

$$\Sigma_+(\zeta) \to O(\zeta^{-1}); \quad U_-(\zeta) \to O(\zeta^{-2}). \tag{96}$$

Nevertheless, active fields exist ahead of the moving crack tip for both mechanical as well as electrical variables, which is a rather curious phenomenon. One of the direct consequences of this "ghost image" is that one may be able to detect a moving crack travelling at a high Mach number speed before it arrives. This may be illustrated through the following example. At $y = 0$, $x > 0$, by using Cagniard–de Hoop scheme, one can set

$$\zeta_+ = -t/x. \tag{97}$$

Based on solution (95), the longitudinal shear strain ahead of the crack can then be measured by the following closed form expression

$$\begin{aligned} \frac{\partial w}{\partial y}(x,0,t) &= -\frac{1}{\pi}\mathrm{Im}\left[\alpha(\zeta_+)U_-(\zeta_+)\frac{\partial\zeta_+}{\partial t}\right] \\ &= P_0\frac{k_v^2}{\pi}\frac{\mathscr{D}_-^{(s)}(-t/x)}{(x+tv)}\frac{D_+^{(s)}(1/v)}{(x+vt)}\left[\frac{v-c}{v+c}\right]^{k_1}\frac{\mathscr{D}_-^{(s)}(-t/x)}{(v-c_{bg})^{2k_1}(v+c_{bg})^{2k_2}} \\ &\quad\cdot\frac{(x+(v+c)t)^{1/2+k_1}(x+(v-c)t)^{1/2-k_1}}{(x+(v+c_{bg})t)^{2k_1}(x+(v-c_{bg})t)^{2k_2}}. \end{aligned} \tag{98}$$

It is worth noting that in (98) as $x \to \infty$ or $t \to \infty$

$$\frac{\partial w}{\partial y}(x,0,t) \to 0, \tag{99}$$

the strain field ahead of crack tip is ephemeral. However, a nonzero strain field is measurable as a crack begins to propagate, even if an observer is far away from the crack tip. This phenomenon is obviously a direct result of piezoelectric behavior.

4. CRACK PROPAGATION UNDER MIXED LOADING

So far in this paper, and in Part I, the focus has been on one facet of the coupling between mechanical and electrical fields intrinsic to piezoelectricity: the generation of electric effects by stress loading. In this section another facet is investigated: the effect of electrical loading. In fact, it turns out to be convenient to examine propagation under general mixed applied load conditions.

As hinted in the discussion at the end of the preceding section, there are reasons to expect some interesting effects, because of the instantaneous (in our model) propagation of electrostatic effects. Indeed, as will be seen, the character of the near-tip fields changes in all three speed regimes under mixed loadings.

4.1. *Integral equation formulation*

The boundary conditions for the mixed loading fundamental problem combine the mechanical conditions from before

$$\sigma_{yz}(x,0^+,t) = -P_0\delta(x+vt)H(t) \quad x<0, \tag{100}$$

$$w(x,0^+,t) = 0 \quad x>0, \tag{101}$$

with the electrical conditions

$$D_y(x,0^+,t)-\tilde{D}_y(x,0^+,t) = -Q_0\delta(x+vt)H(t) \quad x<0, \tag{102}$$

$$E_x(x,0^+,t)-\tilde{E}_x(x,0^+,t) = 0 \quad x<0, \tag{103}$$

$$\phi(x,0^+,t) = 0 \quad x>0. \tag{104}$$

Note that conditions (104) and (101) are deduced from overall antisymmetry.

Although the general solutions given by (30)–(32) still hold, the unknown functions $A(\zeta)$, $B(\zeta)$ and $C(\zeta)$ have to be determined under a different set of boundary conditions into which (102)–(101) may be transformed as follows

$$\begin{cases} \sigma^*_{yz}(x,0^+,p) = -\dfrac{P_0}{v}\exp\left(\dfrac{px}{v}\right) & x<0, \\ w^*(x,0^+,p) = 0 & x>0, \end{cases} \tag{105}$$

$$\begin{cases} D^*_y(x,0^+,p)-\tilde{D}^*_y(x,0^+,p) = -\dfrac{Q_0}{v}\exp\left(\dfrac{px}{v}\right) & x<0, \\ E^*_x(x,0^+,p)-\tilde{E}^*_x(x,0^+,p) = 0 & x<0, \\ \phi^*(x,0^+,p) = 0 & x>0. \end{cases} \tag{106}$$

Because the electrostatic potential in the vacuum area, $\tilde{\phi}$, is not defined in $x>0$, there is an ambiguity in extending the electric boundary condition into the full x range. Consequently, the standard Wiener–Hopf procedure can not be applied to the multiple domain problem directly. Although this can be dealt with by further

manipulations, an alternative approach using integral equations provides a convenient way of reducing the problem.

Substituting the unknown functions $A(\zeta)$, $B(\zeta)$ and $C(\zeta)$ back into (105) and (106) yields a quintuple integral equations, i.e.

$$\begin{cases} \dfrac{1}{2\pi i}\displaystyle\int_{\zeta_c-i\infty}^{\zeta_c+i\infty} [\bar{c}_{44}\alpha(\zeta)A(\zeta)+e_{15}\beta(\zeta)B(\zeta)]\exp(p\zeta x)\,d\zeta = \frac{P_0}{v}\exp\left(\frac{px}{v}\right), & x<0, \quad \text{(a)} \\ \dfrac{1}{2\pi ip}\displaystyle\int_{\zeta_c-i\infty}^{\zeta_c+i\infty} A(\zeta)\exp(p\zeta x)\,d\zeta = 0, & x>0, \quad \text{(b)} \\ \dfrac{1}{2\pi i}\displaystyle\int_{\zeta_c-i\infty}^{\zeta_c+i\infty} [\varepsilon_{11}\beta(\zeta)B(\zeta)+\varepsilon_0\beta(\zeta)C(\zeta)]\exp(p\zeta x)\,d\zeta = -\frac{Q_0}{v}\exp\left(\frac{px}{v}\right), & x<0, \quad \text{(c)} \\ \dfrac{1}{2\pi i}\displaystyle\int_{\zeta_c+i\infty}^{\zeta_c+i\infty} \left[\frac{e_{15}}{\varepsilon_{11}}\zeta A(\zeta)+\zeta B(\zeta)-\zeta C(\zeta)\right]\exp(p\zeta x)\,d\zeta = 0, & x<0, \quad \text{(d)} \\ \dfrac{1}{2\pi ip}\displaystyle\int_{\zeta_c-i\infty}^{\zeta_c+i\infty} B(\zeta)\exp(p\zeta x)\,d\zeta = 0, & x>0, \quad \text{(e)} \end{cases} \tag{107}$$

where

$$-\varepsilon < \mathrm{Re}(\zeta_c) < \varepsilon. \tag{108}$$

From (107d), one can deduce that

$$C(\zeta) = \frac{e_{15}}{\varepsilon_{11}}A(\zeta)+B(\zeta). \tag{109}$$

Inserting (109) back into (107c) yields

$$\frac{1}{2\pi i}\int_{\zeta_c-i\infty}^{\zeta_c+i\infty} \beta(\zeta)\left[\frac{\varepsilon_0 e_{15}}{\varepsilon_{11}}A(\zeta)+(\varepsilon_{11}+\varepsilon_0)B(\zeta)\right]\exp(p\zeta x)\,d\zeta = -\frac{Q_0}{v}\exp\left(\frac{px}{v}\right), \quad x<0. \tag{110}$$

Let

$$R(\zeta) \triangleq \frac{\varepsilon_0 e_{15}}{\varepsilon_{11}}A(\zeta)+(\varepsilon_{11}+\varepsilon_0)B(\zeta). \tag{111}$$

The original quintuple system can then be broken into two dual integral equations with only two unknown functions, $A(\zeta)$ and $R(\zeta)$,

$$\begin{cases} \dfrac{1}{2\pi i}\displaystyle\int_{\zeta_c-i\infty}^{\zeta_c+i\infty} [\alpha(\zeta)-k_v^2\beta(\zeta)]A(\zeta)\exp(p\zeta x)\,d\zeta = \frac{L(P_0,Q_0)}{v}\exp\left(\frac{px}{v}\right), & x<0, \quad \text{(a)} \\ \dfrac{1}{2\pi ip}\displaystyle\int_{\zeta_c-i\infty}^{\zeta_c+i\infty} A(\zeta)\exp(p\zeta x)\,d\zeta = 0, & x>0, \quad \text{(b)} \end{cases} \tag{112}$$

and

$$\begin{cases} \dfrac{1}{2\pi i}\displaystyle\int_{\zeta_c-i\infty}^{\zeta_c+i\infty} \beta(\zeta)R(\zeta)\exp(p\zeta x)\,d\zeta = -\frac{Q_0}{v}\exp\left(\frac{px}{v}\right), & x<0, \quad \text{(a)} \\ \dfrac{1}{2\pi i p}\displaystyle\int_{\zeta_c-i\infty}^{\zeta_c+i\infty} R(\zeta)\exp(p\zeta x)\,d\zeta = 0, & x>0. \quad \text{(b)} \end{cases} \tag{113}$$

In (112), the mixed load factor $L(P_0, Q_0)$ is defined by

$$L(P_0, Q_0) \triangleq \frac{1}{\bar{c}_{44}}\left(P_0 + \frac{e_{15}Q_0}{(\varepsilon_{11}+\varepsilon_0)}\right). \tag{114}$$

The dual integral equation (112) has the same structure as the Wiener–Hopf equation encountered in the preceding section. The solution can then be written down immediately for each crack speed regime.

For $v < c_{bg}$:

$$A_-(\zeta) = -\frac{1}{\sqrt{v}}\frac{(s+k_v^2)}{(1-k_v^4)}\frac{L(P_0,Q_0)}{\sqrt{1-v/c}}\frac{\mathscr{D}_-(\zeta)}{(\zeta-1/v)}\frac{\sqrt{1/(c+v)-\zeta}}{(1/(c_{bg}+v)-\zeta)}. \tag{115}$$

For $c_{bg} < v < c$:

$$A_-(\zeta) = -i\frac{L(P_0,Q_0)}{(c_{bg}+v)}\frac{c^2(s+k_v^2)}{v(\zeta-1/v)}\frac{D_+^{(t)}(1/v)}{(1-(v-c_{bg})\zeta)}\mathscr{D}_-^{(t)}(\zeta). \tag{116}$$

For $c_{bg} < v < c$:

$$A_-(\zeta) = -\frac{L(P_0,Q_0)}{v(\zeta-1/v)}\frac{D_+^{(s)}(1/v)}{(\kappa-ik_v^2)}\left(\frac{1/(v+c)-\zeta}{1/(v-c)-\zeta}\right)^{k_1} \cdot \frac{\mathscr{D}_-^{(s)}(\zeta)}{(1/(v-c_{bg})-\zeta)^{1-2k_1}(1/(v+c_{bg})-\zeta)^{2k_1}}. \tag{117}$$

On the other hand, the dual integral equation (113) needs extra care. The solution procedure outlined here is followed from Sih and Chen (1977).

By Cauchy's integral formula

$$-2\pi i\exp\left(\frac{px}{v}\right) = \int_{\zeta_c-i\infty}^{\zeta_c-i\infty}\frac{H_+(\zeta)}{H_+(1/v)(\zeta-1/v)}\exp(p\zeta x)\,d\zeta, \tag{118}$$

where $H_+(\zeta)$ is an unknown, sectionally analytic function in the half $P_+(\zeta)$ plane.

Thus (113a) can be written as

$$\int_{\zeta_c-i\infty}^{\zeta_c+i\infty}\left\{\beta(\zeta)R_-(\zeta) - \frac{Q_0}{v(\zeta-1/v)}\frac{H_+(\zeta)}{H_+(1/v)}\right\}\exp(p\zeta x)\,d\zeta = 0, \quad x<0. \tag{119}$$

Consequently

$$R_-(\zeta) = -\frac{Q_0 H_+(\zeta)}{vH_+(1/v)(\zeta - 1/v)\beta_+(\zeta)\beta_-(\zeta)}, \tag{120}$$

where

$$\beta_+(\zeta) = \sqrt{\varepsilon + \zeta}, \quad \text{and} \quad \beta_-(\zeta) = \sqrt{\varepsilon - \zeta}. \tag{121}$$

Then the unknown function $H_+(\zeta)$ must have the form

$$H_+(\zeta) = \beta_+(\zeta)P(\zeta), \tag{122}$$

where $P(\zeta)$ is an entire function.

Considering asymptotic behaviors of $R_-(\zeta)$ shows that this entire function can only be unity. It follows that

$$R_-(\zeta) = \frac{Q_0}{\sqrt{v}} \frac{1}{(\zeta - 1/v)} \frac{1}{\sqrt{\varepsilon - \zeta}}. \tag{123}$$

It is important to note that the form of the sectionally analytic function $R_-(\zeta)$ does not change with crack speed regime, in contrast to the function $A_-(\zeta)$. Using the definition of R_-, we finally obtain

$$B_-(\zeta) = \frac{Q_0}{(\varepsilon_{11} + \varepsilon_0)} \frac{1}{\sqrt{v}} \frac{1}{(\zeta - 1/v)} \frac{1}{\sqrt{\varepsilon - \zeta}} - \frac{\bar{c}_{44}}{e_{15}} k_v^2 A_-(\zeta). \tag{124}$$

From (124), it is clear that the sectionally analytic function $B_-(\zeta)$ has two parts: the first represents the instantaneous response to electric loading (unaffected by electroacoustic wave speed); the second is the contribution from mechanical effects (sensitive to electroacoustic wave speed). The implication of this solution under mixed loading conditions is that the stress field and the electric displacement field (but not strain field!) remain singular after the crack extension velocity enters the post-Bleustein–Gulyaev speed region, because the electrostatic effects are instantaneous, and they always outrun the acoustic waves.

4.2. *Closed form solutions*

The development of the preceding subsections provides the basis for more detailed results. Since crack propagation at sub-Bleustein–Galyaev speed is of primary interest, only the subcritical case $v < c_{bg}$ is considered here.

The integral representations of the relevant physical quantities are

$$\sigma_{xz}^*(x, y, t) = \frac{1}{2\pi i}\left\{\bar{c}_{44}\left(\int_{\zeta_\alpha - i\infty}^{\zeta_\alpha + i\infty} \zeta A_-(\zeta) \exp\left[-p(\alpha y - \zeta x)\right] d\zeta \right.\right.$$

$$\left. - k_v^2 \int_{\zeta_\beta - i\infty}^{\zeta_\beta + i\infty} \zeta A_-(\zeta) \exp\left[-p(\beta y - \zeta x)\right] d\zeta \right)$$

$$\left. + \frac{Q_0 e_{15}}{(\varepsilon_{11} + \varepsilon_0)} \frac{1}{\sqrt{v}} \int_{\zeta_\alpha - i\infty}^{\zeta_\alpha + i\infty} \frac{\zeta}{(\zeta - 1/v)} \frac{1}{\sqrt{\varepsilon - \zeta}} \exp\left[-p(\alpha y - \zeta x)\right] d\zeta \right\}, \tag{125}$$

$$\sigma^*_{yz}(x,y,t) = -\frac{1}{2\pi i}\left\{\bar{c}_{44}\left(\int_{\zeta_\alpha-i\infty}^{\zeta_\alpha+i\infty}\alpha(\zeta)A_-(\zeta)\exp\left[-p(\alpha y-\zeta x)\right]d\zeta\right.\right.$$
$$\left.-k_v^2\int_{\zeta_\beta-i\infty}^{\zeta_\beta+i\infty}\beta(\zeta)A_-(\zeta)\exp\left[-p(\beta y-\zeta x)\right]d\zeta\right)$$
$$\left.+\frac{Q_0 e_{15}}{(\varepsilon_{11}+\varepsilon_0)}\frac{1}{\sqrt{v}}\int_{\zeta_\alpha-i\infty}^{\zeta_\alpha+i\infty}\frac{\sqrt{\varepsilon+\zeta}}{(\zeta-1/v)}\exp\left[-p(\alpha y-\zeta x)\right]d\zeta\right\}, \quad (126)$$

$$D^*_x(x,y,p) = \frac{1}{2\pi i}\left\{\frac{\bar{c}_{44}\varepsilon_{11}}{e_{15}}k_v^2\int_{\zeta_\beta-i\infty}^{\zeta_\beta+i\infty}\zeta A_-(\zeta)\exp\left[-p(\beta y-\zeta x)\right]d\zeta\right.$$
$$\left.-\frac{Q_0\varepsilon_{11}}{\varepsilon_{11}+\varepsilon_0}\int_{\zeta_\beta-i\infty}^{\zeta_\beta+i\infty}\frac{\zeta}{(\zeta-1/v)}\frac{1}{\sqrt{\varepsilon-\zeta}}\exp\left[-p(\beta y-\zeta x)\right]d\zeta\right\}, \quad (127)$$

$$D^*_y(x,y,p) = -\frac{1}{2\pi i}\left\{\frac{\bar{c}_{44}\varepsilon_{11}}{e_{15}}k_v^2\int_{\zeta_\beta-i\infty}^{\zeta_\beta+i\infty}\beta(\zeta)A_-(\zeta)\exp\left[-p(\beta y-\zeta x)\right]d\zeta\right.$$
$$\left.-\frac{Q_0\varepsilon_{11}}{\varepsilon_{11}+\varepsilon_0}\int_{\zeta_\beta-i\infty}^{\zeta_\beta+i\infty}\frac{\sqrt{\varepsilon+\zeta}}{(\zeta-1/v)}\exp\left[-p(\beta y-\zeta x)\right]d\zeta\right\}. \quad (128)$$

For the anti-plane displacement and the in-plane electric fields, we have

$$w^*(x,y,p) = \frac{1}{2\pi p}\int_{\zeta_\alpha-i\infty}^{\zeta_\alpha+i\infty}A_-(\zeta)\exp\left[-p(\alpha y-\zeta x)\right]d\zeta, \quad (129)$$

$$\psi^*(x,y,p) = \frac{1}{2\pi i p}\left\{-\frac{\bar{c}_{44}}{e_{15}}k_v^2\int_{\zeta_\beta-i\infty}^{\zeta_\beta+i\infty}A_-(\zeta)\exp\left[-p(\beta y-\zeta x)\right]d\zeta\right.$$
$$\left.+\frac{Q_0}{(\varepsilon_{11}+\varepsilon_0)}\frac{1}{\sqrt{v}}\int_{\zeta_\beta-i\infty}^{\zeta_\beta+i\infty}\frac{1}{(\zeta-1/v)\sqrt{\varepsilon-\zeta}}\exp\left[-p(\beta y-\zeta x)\right]d\zeta\right\}, \quad (130)$$

$$\phi^*(x,y,p) = \frac{1}{2\pi i p}\left\{\frac{\bar{c}_{44}}{e_{15}}\left(k_e^2\int_{\zeta_\alpha-i\infty}^{\zeta_\alpha+i\infty}A_-(\zeta)\exp\left[-p(\alpha y-\zeta x)\right]d\zeta\right.\right.$$
$$\left.-k_v^2\int_{\zeta_\beta-i\infty}^{\zeta_\beta+i\infty}A_-(\zeta)\exp\left[-p(\beta y-\zeta x)\right]d\zeta\right)$$
$$\left.+\frac{Q_0}{(\varepsilon_{11}+\varepsilon_0)}\frac{1}{\sqrt{v}}\int_{\zeta_\beta-i\infty}^{\zeta_\beta+i\infty}\frac{1}{(\zeta-1/v)\sqrt{\varepsilon-\zeta}}\exp\left[-p(\beta y-\zeta x)\right]d\zeta\right\}, \quad (131)$$

$$\tilde{\phi}^*(x,y,p) = \frac{1}{2\pi i p}\left\{\frac{e_{15}}{(\varepsilon_{11}+\varepsilon_0)}\int_{\zeta_\beta-i\infty}^{\zeta_\beta+i\infty}A_-(\zeta)\exp\left[p(\beta y-\zeta x)\right]d\zeta\right.$$
$$\left.+\frac{Q_0}{(\varepsilon_{11}+\varepsilon_0)}\frac{1}{\sqrt{v}}\int_{\zeta_\beta-i\infty}^{\zeta_\beta+i\infty}\frac{1}{(\zeta-1/v)\sqrt{\varepsilon-\zeta}}\exp\left[p(\beta y-\zeta x)\right]d\zeta\right\}. \quad (132)$$

The above are the general solutions for the moving piezoelectric crack under mixed loading conditions, valid for the whole range of crack propagation velocity. The Cagniard–de Hoop inversion scheme can be used to find closed form solutions by employing the following inversion paths

$$\zeta_{1+}(x,t)=\frac{1}{x^2+s^2y^2}\left(-\left(xt+\frac{v}{c^2}\right)+\mathrm{i}y\sqrt{s^2t^2-\frac{2v}{c^2}xt-\frac{r^2}{c^2}}\right), \tag{133}$$

$$\zeta_{2+}(x,t)=\frac{1}{x^2+y^2}\left(-xt+\mathrm{i}yt\sqrt{1-e^2\frac{v^2}{t^2}}\right). \tag{134}$$

For $v < c_{bg}$, it follows that

$$\begin{aligned}\sigma_{xz}(x,y,t)=\frac{1}{\pi}\Bigg\{\bar{c}_{44}\Bigg(&\mathrm{Im}\left[\zeta_{1+}A_-(\zeta_{1+})\frac{\partial\zeta_{1+}}{\partial t}\right]H(t-t_1)\\&-k_v^2\,\mathrm{Im}\left[\zeta_{2+}A_-(\zeta_{2+})\frac{\partial\zeta_{2+}}{\partial t}\right]H(t-t_2)\Bigg)\\&+\frac{Q_0e_{15}}{(\varepsilon_{11}+\varepsilon_0)}\frac{1}{\sqrt{v}}\mathrm{Im}\left[\frac{\zeta_{2+}}{(\zeta_{2+}-1/v)}\frac{1}{\sqrt{\varepsilon-\zeta_{2+}}}\frac{\partial\zeta_{2+}}{\partial t}\right]H(t-t_2)\Bigg\},\end{aligned} \tag{135}$$

$$\begin{aligned}\sigma_{yz}(x,y,t)=-\frac{1}{\pi}\Bigg\{\bar{c}_{44}\Bigg(&\mathrm{Im}\left[\alpha(\zeta_{1+})A_-(\zeta_{1+})\frac{\partial\zeta_{1+}}{\partial t}\right]H(t-t_1)\\&-k_v^2\,\mathrm{Im}\left[\beta(\zeta_{2+})A_-(\zeta_{2+})\frac{\partial\zeta_{2+}}{\partial t}\right]H(t-t_2)\Bigg)\\&+\frac{Q_0e_{15}}{(\varepsilon_{11}+\varepsilon_0)}\mathrm{Im}\left[\frac{\sqrt{\varepsilon+\zeta_{2+}}}{(\zeta_{2+}-1/v)}\frac{\partial\zeta_{2+}}{\partial t}\right]H(t-t_2)\Bigg\},\end{aligned} \tag{136}$$

$$\begin{aligned}D_x(x,y,t)=\frac{1}{\pi}\Bigg\{&\frac{e_{15}\bar{c}_{44}}{\varepsilon_{11}}k_v^2\,\mathrm{Im}\left[\zeta_{2+}A_-(\zeta_{2+})\frac{\partial\zeta_{2+}}{\partial t}\right]H(t-t_2)\\&-\frac{Q_0}{\sqrt{v}}\frac{\varepsilon_{11}}{(\varepsilon_{11}+\varepsilon_0)}\mathrm{Im}\left[\frac{\zeta_{2+}}{(\zeta_{2+}-1/v)}\frac{1}{\sqrt{\varepsilon-\zeta_{2+}}}\frac{\partial\zeta_{2+}}{\partial t}\right]H(t-t_2)\Bigg\},\end{aligned} \tag{137}$$

$$\begin{aligned}D_y(x,y,t)=-\frac{1}{\pi}\Bigg\{&\frac{e_{15}\bar{c}_{44}}{\varepsilon_{11}}k_v^2\,\mathrm{Im}\left[\beta(\zeta_{2+})A_-(\zeta_{2+})\frac{\partial\zeta_{2+}}{\partial t}\right]H(t-t_2)\\&-\frac{Q_0}{\sqrt{v}}\frac{\varepsilon_{11}}{(\varepsilon_{11}+\varepsilon_0)}\mathrm{Im}\left[\frac{\sqrt{\varepsilon+\zeta_{2+}}}{(\zeta_{2+}-1/v)}\frac{\partial\zeta_{2+}}{\partial t}\right]H(t-t_2)\Bigg\},\end{aligned} \tag{138}$$

where

$$\begin{cases} t_1 = \dfrac{1}{s^2}\left[\dfrac{vx}{c^2} + \dfrac{1}{c}\sqrt{x^2+s^2y^2}\right], \\ t_2 = \varepsilon r. \end{cases} \tag{139}$$

In particular, ahead of the crack tip ($y = 0, x > 0$), when $t > t_1$ and $x < (c-v)t$, the electro-mechanical fields can be expressed in elementary forms

$$\sigma_{yz}(x, 0^+, t) = [s\sqrt{(t-x/(c-v))(t+x/(c+v))} - k_v^2 t]\mathscr{M}(x,t) - \frac{1}{\pi}\frac{Q_0}{\sqrt{v}}\frac{e_{15}}{(\varepsilon_{11}+\varepsilon_0)}\frac{1}{(t+x/v)}\sqrt{\frac{t}{x}}, \tag{140}$$

$$D_y(x, 0^+, t) = \frac{\varepsilon_{11}}{e_{15}}k_v^2\mathscr{M}(x,t) + \frac{1}{\pi}\frac{Q_0}{\sqrt{v}}\frac{\varepsilon_{11}}{(\varepsilon_{11}+\varepsilon_0)}\frac{1}{(t+x/v)}\sqrt{\frac{t}{x}}, \tag{141}$$

where

$$\mathscr{M}(x,t) \triangleq \frac{1}{\pi}\frac{(s+k_v^2)}{(1-k_v^4)}\frac{\tilde{L}(P_0,Q_0)}{\sqrt{1-v/c}}\frac{\sqrt{t+x/(c+v)}}{(t+x/(c_{bg}+v))}\frac{\mathscr{D}_+(1/v)}{(1+v/c_{bg})}\cdot\frac{\mathscr{D}_-(-t/x)}{(t+x/v)}\frac{H(t-t_1)}{\sqrt{vx}}, \tag{142}$$

and

$$\tilde{L}(P_0,Q_0) \triangleq P_0 + \frac{e_{15}}{(\varepsilon_{11}+\varepsilon_0)}Q_0. \tag{143}$$

As $x \to 0^+$, the near field solutions can be directly obtained from (140) and (141) as

$$\sigma_{yz}(x,0^+,t) = \left(\frac{(1-v/c_{bg})}{\sqrt{1-v/c}}\mathscr{D}_+(1/v)\right)\left[\frac{1}{\pi}\frac{P_0}{\sqrt{vxt}}\right] + \left(\frac{(1-v/c_{bg})}{\sqrt{1-v/c}}\mathscr{D}_+(1/v)-1\right)\left[\frac{1}{\pi}\frac{Q_0 e_{15}}{(\varepsilon_{11}+\varepsilon_0)}\frac{1}{\sqrt{vxt}}\right] + \mathscr{O}(1), \tag{144}$$

$$D_y(x,0^+,t) = \left(\frac{(s+k_v^2)}{(1+k_v^2)}\frac{1}{\sqrt{1-v/c}}\frac{\mathscr{D}_+(1/v)}{(1+v/c_{bg})}\right)\left[\frac{1}{\pi}\frac{\varepsilon_{11}}{e_{15}}\frac{k_v^2}{(1-k_v^2)}\frac{P_0}{\sqrt{vxt}}\right] + \left(\frac{k_v^2}{(1-k_v^2)}\frac{(s+k_v^2)}{(1+k_v^2)}\frac{k_v^2}{\sqrt{1-v/c}}\frac{\mathscr{D}_+(1/v)}{(1+v/c_{bg})}+1\right) \cdot\left[\frac{1}{\pi}\frac{\varepsilon_{11}}{\varepsilon_{11}+\varepsilon_0}\frac{Q_0}{\sqrt{vxt}}\right] + \mathscr{O}(1). \tag{145}$$

For $v > c_{bg}$, a closed form solution under the mixed type of boundary condition could be derived in a similar fashion. Here we restrict attention to the intensity factors, which can in this case be derived without inversion by applying the Abel theorem

$$\lim_{x\to 0^+}(\pi x)^{1/2}\sigma_{yz}^{*}(x,0,p)=\lim_{\zeta\to+\infty}(p\zeta)^{1/2}\left(\frac{-1}{p}\right)\frac{Q_0e_{15}}{(\varepsilon_0+\varepsilon_{11})}\frac{1}{\sqrt{v}}\frac{\sqrt{\varepsilon+\zeta}}{(\zeta-1/v)}$$

$$=-\frac{Q_0e_{15}}{(\varepsilon_0+\varepsilon_{11})}\frac{1}{\sqrt{vp}}. \tag{146}$$

Slightly anticipating the following section, it follows that the stress intensity factor under mixed loading is

$$K_{III}^{(\sigma)}(vt,v)=-\frac{Q_0e_{15}}{(\varepsilon_0+\varepsilon_{11})}\frac{1}{\sqrt{vt}}. \tag{147}$$

Likewise, the electric displacement intensity factor is

$$K_{III}^{(D)}(vt,v)=\frac{Q_0\varepsilon_{11}}{(\varepsilon_{11}+\varepsilon_0)}\frac{1}{\sqrt{vt}}. \tag{148}$$

These singular fields exist as a result of instantaneous electrostatic response corresponding to the current crack extension vt—note the lack of explicit v dependence. Though the point is not pursued here, it may also be shown that the fields ahead of the crack do not decay with time as they do in the traction loading case.

5. RESULTS AND DISCUSSION

The results of the preceding sections demonstrate the richness of dynamic piezoelectric crack problems. Even in the simple antiplane case, the analysis unearths a variety of phenomena never encountered in the purely mechanical world. In this paper, we restrict attention to a few direct consequences, considering only the subcritical case. Of primary interest are the quantities of traditional interest in dynamic fracture mechanics: intensity factors and energy release rate. In addition, we examine the crack face electrostatic potential distribution.

5.1. *Intensity factors and universal functions*

As shown in the preceding section, the subcritical case is fully coupled, in the sense that applied traction loading and applied electric charge loading each produce singular near-tip fields for both stress and electric displacement. We introduce some terminology and notation to carefully characterize the various interactions. In particular, we distinguish a self-induced *intensity factor* (generated by a loading of the same type) from a *cross-over intensity factor* (generated by a loading of the other type).

More precisely, separating the mixed loading solution into parts corresponding to the different types of loading, we may define

$$\sigma_{yz}^{(p)}(x,y,t)\triangleq\sigma_{yz}(x,y,t)\Big|_{\substack{P_0=1,\\ Q_0=0}} \tag{149}$$

$$\sigma_{yz}^{(g)}(x,y,t) \triangleq \sigma_{yz}(x,y,t)\Big|_{\substack{P_0=0,\\ Q_0=1}} \tag{150}$$

$$D_y^{(p)}(x,y,t) \triangleq D_y(x,y,t)\Big|_{\substack{P_0=1,\\ Q_0=0}} \tag{151}$$

$$D_y^{(g)}(x,y,t) \triangleq D_y(x,y,t)\Big|_{\substack{P_0=0.\\ Q_0=1}} \tag{152}$$

Taking the opportunity to generalize the results in the manner of Freund (1972) let $p(X)$ describe a traction distribution that appears on the newly formed crack faces. The self-induced stress intensity factor [denoted by superscript (σ) and subscript T] may then be expressed as

$$K_{III}^{(\sigma)}(vt,v) \triangleq \lim_{x\to 0}\sqrt{2\pi x}\int_0^{vt}\sigma_{yz}^{(p)}(x,0^+,t-X/v)p(X)\,\mathrm{d}X$$

$$=\left(\frac{(1-v/c_{bg})}{\sqrt{1-v/c}}\mathscr{D}_+(1/v)\right)P(vt), \tag{153}$$

where

$$P(l)=\sqrt{\frac{2}{\pi}}\int_0^l \eta^{-1/2}p(l-\eta)\,\mathrm{d}\eta. \tag{154}$$

Similarly, let $q(X)$ describe a charge distribution that appears on the newly formed crack faces. The cross-over stress intensity factor [denoted by superscript (σ) and subscript D] is then given by

$$K_{IID}^{(\sigma)}(vt,v) \triangleq \lim_{x\to 0}\sqrt{2\pi x}\int_0^{vt}\sigma_{yz}^{(g)}(x,0^+,t-X/v)q(X)\,\mathrm{d}X$$

$$=\left(\frac{(1-v/c_{bg})}{\sqrt{(1-v/c)}}\mathscr{D}_+(1/v)-1\right)\frac{e_{15}}{(\varepsilon_{11}+\varepsilon_0)}Q(vt), \tag{155}$$

where

$$Q(l)=\sqrt{\frac{2}{\pi}}\int_0^l \eta^{-1/2}q(l-\eta)\,\mathrm{d}\eta. \tag{156}$$

The self-induced and cross-over electric displacement factors may be similarly defined [denoted by superscript (D) and respective subscripts D and T] and expressed as

$$K_{IID}^{(D)}(vt,v) \triangleq \lim_{x\to 0}\sqrt{2\pi x}\int_0^{vt}D_y^{(g)}(x,0,t-X/v)q(X)\,\mathrm{d}X$$

$$=\left(\frac{(s+k_v^2)}{(1-k_v^4)}\frac{k_v^2}{\sqrt{(1-v/c)}}\frac{\mathscr{D}_+(1/v)}{(1+v/c_{bg})}+1\right)\frac{\varepsilon_{11}}{\varepsilon_{11}+\varepsilon_0}Q(vt) \tag{157}$$

and

$$K_{IIIT}^{(D)}(vt,v) \triangleq \lim_{x\to 0}\sqrt{2\pi x}\int_0^{vt} D_y^{(p)}(x,0,t-X/v)p(X)\,\mathrm{d}X$$

$$=\left(\frac{(s+k_v^2)}{(1+k_v^2)}\frac{1}{\sqrt{(1-v/c)}}\frac{\mathscr{D}_+(1/v)}{(1+v/c_{bg})}\right)\frac{\varepsilon_{11}}{e_{15}}\frac{k_v^2}{(1-k_v^2)}P(vt). \tag{158}$$

A similar cross-over electric displacement intensity factor was defined for the "electrode" solution in Part I. For that case, the nonvanishing cross-over electric displacement intensity factor was unimportant as far as energy release rate was concerned; as we shall see, this is not the case in general.

It is important to note that the structure of the asymptotic fields is not as straightforward as the electrode case, thanks to the existence of two different terms (though both are square root singular). Rather than pursue this parameterization here, universal crack speed factors are expressed in terms of the loadings P and Q. The four such functions necessary for this case may be chosen to satisfy

$$\begin{cases} K_{IIIT}^{(\sigma)}(vt,v) = f_s(v)P(vt), \\ K_{IIID}^{(\sigma)}(vt,v) = f_c(v)\dfrac{e_{15}}{(\varepsilon_{11}+\varepsilon_0)}Q(vt), \end{cases} \tag{159}$$

$$\begin{cases} K_{IIID}^{(D)}(vt,v) = g_s(v)\dfrac{\varepsilon_{11}}{(\varepsilon_{11}+\varepsilon_0)}Q(vt), \\ K_{IIIT}^{(D)}(vt,v) = g_c(v)\dfrac{\varepsilon_{11}}{e_{15}}\dfrac{k_v^2}{(1-k_v^2)}P(vt). \end{cases} \tag{160}$$

These functions may be expressed in terms of the universal functions f and g derived for the electrode case in Part I† as

$$f_s(v) = f(v), \tag{161}$$

$$f_c(v) = f(v)-1, \tag{162}$$

$$g_s(v) = \frac{k_v^2}{1-k_v^2}g(v)+1, \tag{163}$$

$$g_c(v) = g(v), \tag{164}$$

where

$$f(v) \triangleq \frac{(1-v/c_{bg})}{\sqrt{(1-v/c)}}\mathscr{D}_+(1/v), \tag{165}$$

$$g(v) \triangleq \frac{(s+k_v^2)}{(1+k_v^2)}\frac{1}{\sqrt{(1-v/c)}}\frac{\mathscr{D}_+(1/v)}{(1+v/c_{bg})}. \tag{166}$$

† With the understanding that the electrode values for Bleustein–Gulyaev speed and electromechanical coupling are replaced by the corresponding vacuum values.

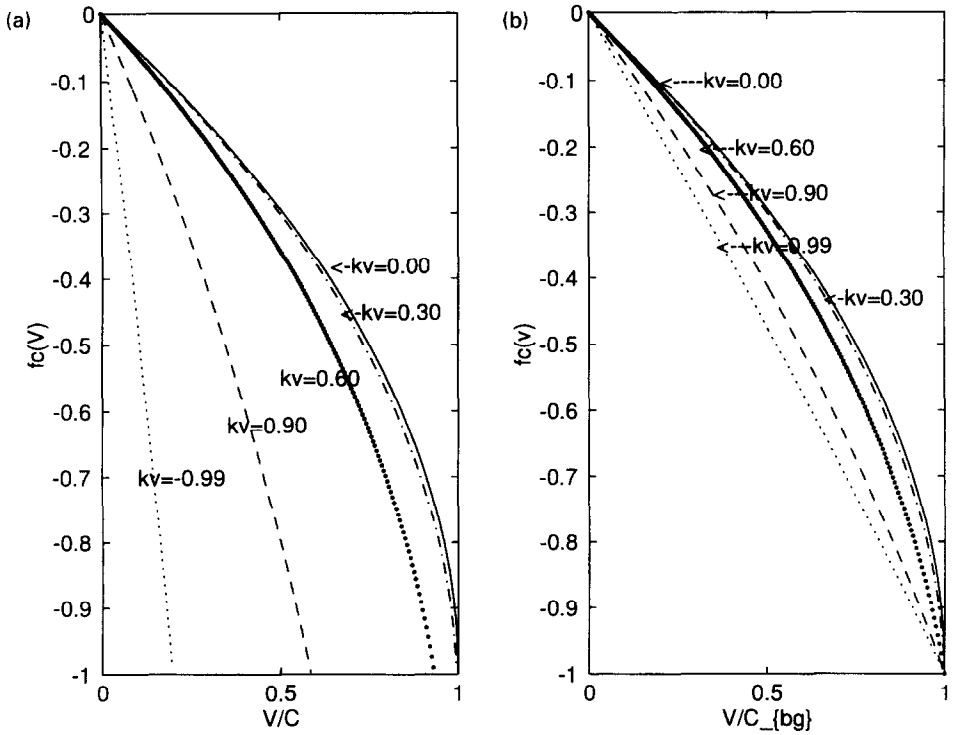

Fig. 6. Variation of cross-over dynamic stress intensity factor $f_c(v)$ with nondimensional crack velocities: (a) $f_c(v)$ vs v/c; (b) $f_c(v)$ vs v/c_{bg}.

In Part I, $f(v)$ and $g(v)$ were plotted for various electro-mechanical coefficients. In Fig. 6, the cross-over dynamic stress intensity factor $f_c(v)$ is similarly plotted against two nondimensional crack speeds; the results of course only differ by a constant from those for f. Note that f_c is zero at $v = 0$. Figure 7 displays the profile of self-induced electric displacement intensity factor, $g_s(v)$. In the acoustic speed range, this factor is always greater than one.

An important practical observation is that typical values of k_v are much smaller than those for k_e. The variations in intensity factor with velocity, the reduction in Bleustein–Gulyaev wave speed and the cross-over factors are thus substantially smaller for realistic material parameters than in the electrode case.

5.1.1. *New static solution.* A slight digression is in order to examine further the limiting case $v = 0$. Most published static analyses of piezoelectric crack problems adopt the assumption that the crack contains a dielectrically impermeable medium. This assumption is analytically useful in that the field equations no longer couple via the interfacial conditions at the crack faces, allowing significant simplification. An immediate corollary, however, is the lack of any cross-over terms.

In contrast, the quasi-static ($v \to 0$) limit of the present results, which may be interpreted as the intensity factors for a static semi-infinite crack with mixed loading on the crack faces in the region $-l < x < 0$, yields

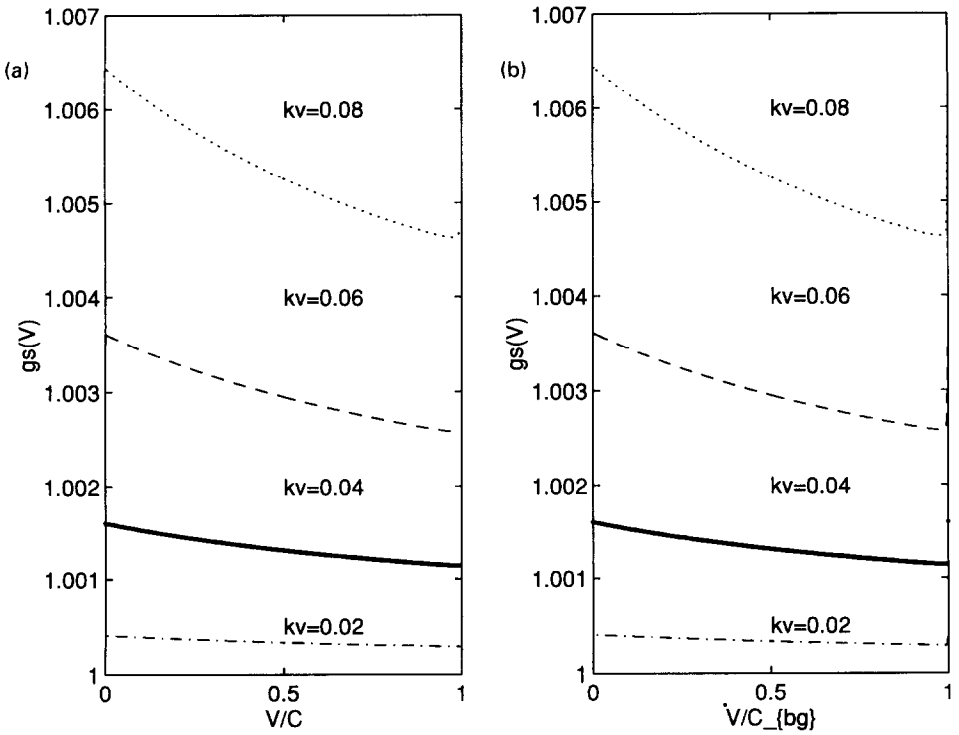

Fig. 7. Variation of self-induced dynamic electric displacement intensity factors with nondimensional crack velocities: (a) $g_s(v)$ vs v/c; (b) $g_s(v)$ vs v/c_{bg}.

$$K_{IIIT}^{(\sigma)} = P(l), \tag{167}$$

$$K_{IIID}^{(\sigma)} = 0, \tag{168}$$

$$K_{IIID}^{(D)} = \frac{1}{(1-k_v^2)} \frac{\varepsilon_{11}}{(\varepsilon_{11}+\varepsilon_0)} Q(l), \tag{169}$$

$$K_{IIIT}^{(D)} = \frac{\varepsilon_{11}}{e_{15}} \frac{k_v^2}{(1-k_v^2)} P(l). \tag{170}$$

Thus, for the permeable case, a cross-over electric displacement intensity factor exists. The impermeable case is recovered in the limit $\varepsilon_0 \to 0$, when $k_v \to 0$ and this term vanishes.

These results allow the validity of the *a priori* assumption of impermeability to be assessed for the static antiplane case. In particular, it is clear that both the perturbation in the self-induced electric displacement intensity factor and the magnitude of the cross-over intensity factor are first order in $\varepsilon_0/\varepsilon_{11}$.

5.2. *Energy release rate*

Energy release rate and the associated path-independent integrals in an elastic dielectric have received significant attention in recent years (Pak and Herrmann,

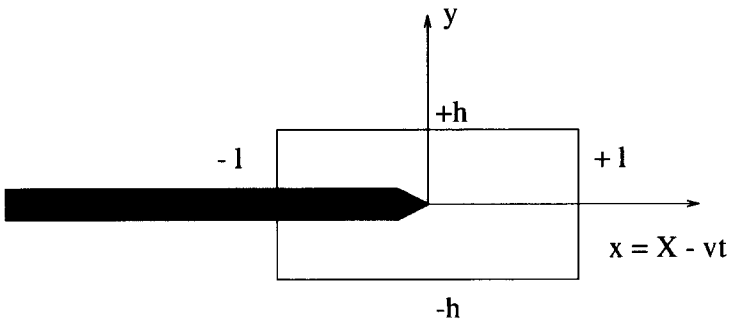

Fig. 8. Integration contour used to evaluate J-integral and energy release rate.

1986a, b; McMeeking, 1990; Maugin and Epstein, 1991; Vukobrat, 1994). Maugin (1994) gives a comprehensive review of the subject. In the static case, some specific calculations have been carried out (Pak, 1992; Zhang and Hack 1992). For dynamic piezoelectric fracture, general treatments of the energy balance have been given (Parton and Kudryatvsev, 1988; Maugin, 1994).

Here it is possible to carry out the detailed calculation of the energy release rate for the antiplane dynamic problem. The starting point is the family of invariant integrals, which for a linear dielectric medium under the quasi-static approximation take the form (Pak, 1990, 1992)

$$F_k = \int_S [H\delta_{jk} - \sigma_{ij}u_{i,k} + D_j E_k]n_j \, \mathrm{d}S, \tag{171}$$

where H is the enthalpy density. When $k = 1$, (171) is the generalized J-integral for an elastic dielectric medium, which includes the linear piezoelectric material as a special case.

By choosing the integration contour S shown in Fig. 8, and allowing the area encircled by S to shrink in the usual way ($h \to 0$, then $\ell \to 0$), the only contribution to the energy release rate is

$$G = J = 2\lim_{\ell \to 0} \int_{-\ell}^{\ell} \left(\sigma_{yz} \frac{\partial w}{\partial x} + D_y \frac{\partial \phi}{\partial x} \right) \mathrm{d}x. \tag{172}$$

The results of the previous section may be employed to express the energy release rate in terms of the load pair as

$$G(vt, v) = \frac{1}{2\bar{c}_{44}} h_{TT}(v)P(vt)P(vt) + \frac{1}{e_{15}} h_{TD}(v)P(vt)Q(vt) + \frac{1}{2(\varepsilon_0 + \varepsilon_{11})} h_{DD}(v)Q(vt)Q(vt), \tag{173}$$

where

$$h_{TT}(v) \triangleq \frac{1}{(1-k_v^2)}\left[f(v)g(v)+g(v)g(v)\frac{k_v^2}{(1-k_v^2)}\frac{\varepsilon_{11}}{(\varepsilon_0+\varepsilon_{11})}\right], \tag{174}$$

$$h_{TD}(v) \triangleq \frac{k_v^2}{(1-k_v^2)}\left[f(v)g(v)+\frac{g(v)g(v)}{(1-k_v^2)}\frac{k_v^2\varepsilon_{11}^2}{\varepsilon_0(\varepsilon_0+\varepsilon_{11})}-\frac{g(v)\varepsilon_{11}}{(\varepsilon_0+\varepsilon_{11})}\right], \tag{175}$$

$$h_{DD}(v) \triangleq h_{TD}(v)-g(v)\frac{k_v^2}{(1-k_v^2)}\frac{\varepsilon_{11}}{(\varepsilon_0+\varepsilon_{11})}-\frac{\varepsilon_{11}}{(\varepsilon_0+\varepsilon_{11})}. \tag{176}$$

For traction loading only, this reduces to

$$G(vt,v)=\frac{1}{2\bar{c}_{44}}h_{TT}(v)P(vt)P(vt). \tag{177}$$

Examination of the two terms in the expression for h_{TT} reveals that as $v \to c_{bg}$, the first term vanishes, but the second does not. Normalizing by

$$G_{00} \triangleq \frac{1}{2\bar{c}_{44}(1-k_v^2)}\left(1+\frac{k_v^2 r}{1-k_v^2}\right)P(vt)P(vt), \tag{178}$$

where $r \triangleq \varepsilon_{11}/(\varepsilon_0+\varepsilon_{11})$, it follows that

$$\frac{G(vt,v)}{G_{00}(vt)}=\left(1+\frac{k_v^2 r}{(1-k_v^2)}\right)^{-1}\left(f(v)g(v)+g(v)g(v)\frac{k_v^2 r}{(1-k_v^2)}\right). \tag{179}$$

This expression is plotted for a realistic value of r in Fig. 9. Clearly, there is a "residual" energy release rate left when crack speed is up to surface wave speed, unlike the elastodynamic and the electrode case previously examined. For the case of the vacuum condition, the surface wave speed does not appear to be a barrier to crack propagation.

The origin of this residual energy release rate needs further investigation. There are several reasons to anticipate novel behavior for the coupled electromechanical problem, but we are only able to speculate as to the detailed mechanisms at this point.

The first observation is that the propagation of electric effects is not limited by acoustic velocities. At the surface wave speed limit, therefore, it is conceivable that there are boundary effects that provide a mechanism for energy flux that does not exist in the purely mechanical cases. Second, unlike either the elastodynamic or the electrode case, the vacuum cavity inside the crack is energetically active, due to the electric field supported within. This field is, in addition, singular as the tip is approached; it is not clear what the consequences of this are for energy exchange between the piezoelectric body and the cavity. It is significant that both of these effects are suppressed by the electrode boundary condition choice.

Here is a possible explanation which offers the authors' viewpoint. As pointed out by Freund (1990) for a crack expanding in purely elastic materials, the energy rate G is called elastic energy release rate only if the crack advances under equilibrium conditions and the fixed grip boundary condition. This so called "*fixed grip*" boundary

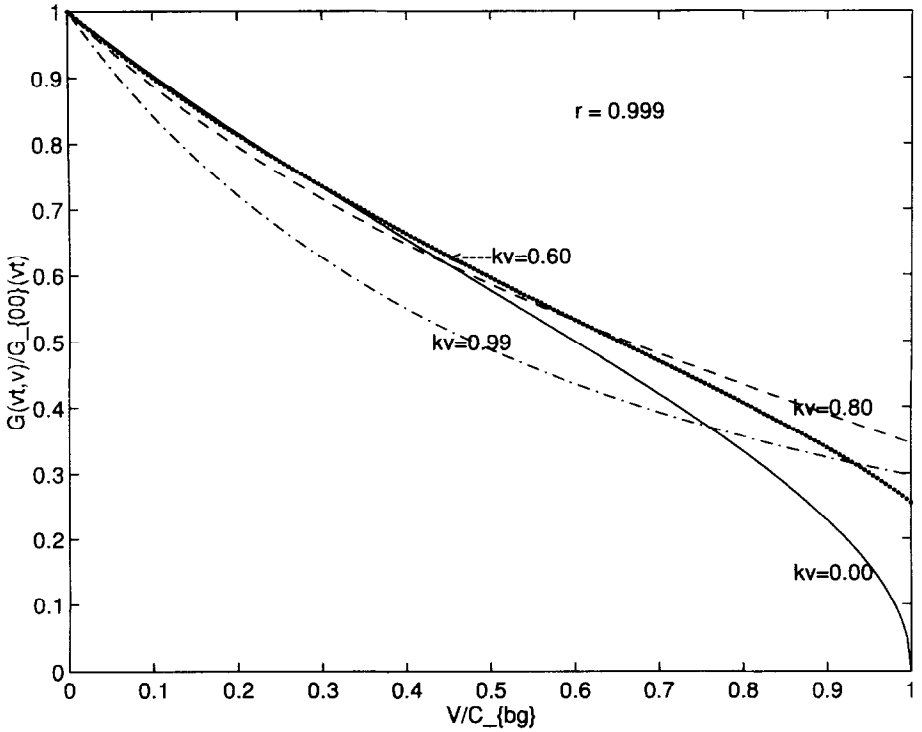

Fig. 9. Normalized energy release versus v/c_{bg}.

condition excludes any exchange of energy between the elastic body and its surroundings.

Obviously, in our case, this "*fixed grip*" condition is violated. As shown in the previous sections there is a continuous energy exchange between the piezoelectric body and its surrounding vacuum space. It can be shown that the electric field in the vacuum region is also singular near the crack tip area as its counterpart in the piezoelectric body. As shown above, the electric displacement intensity factor will not go to zero as the crack speed approaches the Bleustein–Gulyaev speed. In other words, the electrostatic field remains singular when crack speed approaches the surface wave speed whereas the singularity of mechanical fields disappears. Therefore, when crack speed reaches the surface wave speed, there is still electrical energy exchange between the piezoelectric body and its surrounding vacuum space. It is this fact, we believe, that is responsible for the existence of the "*residual*" energy release rate.

On the other hand, in electrode-type boundary problems, we mathematically enforce the "*fixed grip*" condition, i.e. we shut off the energy exchange gate between piezoelectric body and its environment. Thus, the energy release rate always goes to zero when crack propagation speed approaches the Bleustein–Gulyaev speed. Whereas on the contrary, in vacuum boundary problems, we open the energy exchange channel; this is why there is a "*residual*" energy release rate left. The physical meaning of this residual energy release rate is an energy rate supply that piezoelectric body outputs to its vacuum surroundings.

For pure charge loading, there is another interesting effect. If $p(x) = 0$, the energy release rate $G(vt, v)$ can be regrouped into the following form

$$G(vt,v) = \frac{1}{2(\varepsilon_0+\varepsilon_{11})}\left\{g(v)(f(v)-1)\frac{k_v^2}{(1-k_v^2)}\right.$$
$$\left. + \frac{\varepsilon_{11}}{(\varepsilon_{11}+\varepsilon_0)}g_s(v)\left[g(v)\frac{k_e^2}{(1-k_v^2)}\frac{\varepsilon_{11}}{(\varepsilon_{11}+\varepsilon_0)}-1\right]\right\}Q(vt)Q(vt). \tag{180}$$

Since for $v > 0$,

$$f(v)-1 < 0 \tag{181}$$

and in most practically used piezoelectric materials

$$g(v)\frac{\varepsilon_{11}}{(\varepsilon_0+\varepsilon_{11})}\frac{k_e^2}{(1-k_v^2)}-1 < 0. \tag{182}$$

Thus, the energy release rate may be negative. In fact, in the impermeable limit, this term is guaranteed to be negative. This result agrees with the results found in static analysis (Deeg, 1980; Pak, 1990; Maugin, 1994). Maugin notes, "It is found that in some cases the energy release rate can have negative values,.... In addition, in the absence of mechanical loads, it is noted that crack extension force is always negative,...". The same observation was reported by Pak: "it is found that the presence of an electric field always decreases J thus inducing retardation in the crack growth."

5.3. *Electrostatic potential distributions*

Measurement of electrical quantities such as resistance have been occasionally used to monitor fracture. For piezoelectric materials, it would seem reasonable to expect that electrostatic measurements would be particularly useful. As an example, the potential drop across the crack surfaces may be calculated.

Allowing the thickness of the vacuum region to approach zero, the potential jump across the crack is

$$\Delta\tilde{\phi}(x,0^{\pm},t) = [\tilde{\phi}(x,0,t)] \triangleq \tilde{\phi}(x,0^+,t)-\tilde{\phi}(x,0^-,t), \tag{183}$$

or

$$|\Delta\tilde{\phi}(x,0,t)| = 2|\tilde{\phi}(x,0^+,t)|. \tag{184}$$

For simplicity, let $Q_0 = 0$. Then at $y = 0$, from (132), one can obtain

$$\Delta\tilde{\phi}(x,0,t) = \Delta\tilde{\phi}_0\int_{c/(v+c)}^{tc/|x|}\frac{\mathscr{D}_-(\xi/c)}{(\xi-c/v)}\frac{\sqrt{\xi-c/(c+v)}}{(\xi-c/(c_{bg}+v))}\mathrm{d}\xi, \tag{185}$$

where

$$\Delta\tilde{\phi}_0 \triangleq \frac{2}{\pi}\sqrt{\frac{c}{v}}\frac{(s+k_v^2)}{(1-k_v^4)}\frac{P_0}{\sqrt{(1-v/c)}}\frac{\mathscr{D}_+(1/v)}{(1+v/c_{bg})}\frac{\varepsilon_{11}}{\varepsilon_0}\frac{k_v^2}{e_{15}}. \tag{186}$$

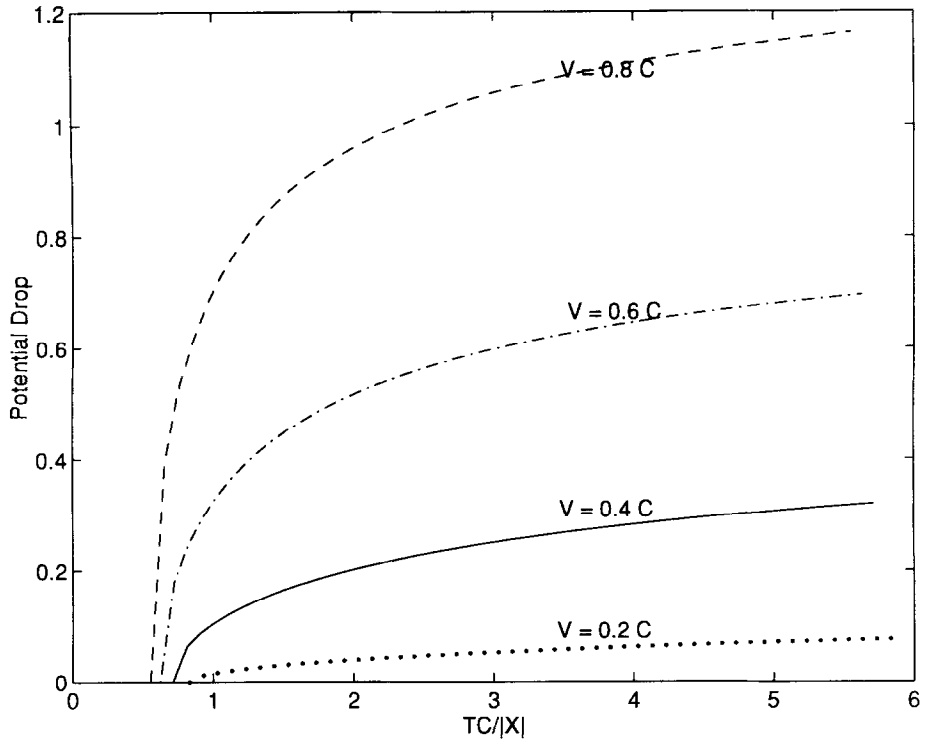

Fig. 10. Normalized potential drop along the crack surfaces.

Figure 10 displays the distribution of the electric potential drop along the crack surface in the range $|x| > (c+v)t$. The normalized electric potential drop is plotted against the nondimensional variable $tc/|x|$.

6. CLOSURE

The closed form solutions obtained here for the anti-plane dynamic piezoelectric crack problem demonstrate some fascinating phenomena, of which the present paper has only scratched the surface. In addition to behavior reminiscent of the in-plane elastic case, we have discovered a variety of truly coupled behavior resulting from the electromechanical properties.

As expected, surface wave phenomena have a critical effect on dynamic piezoelectric fracture. Because of the difference in propagation of electromagnetic (quasi-static) and acoustic disturbances, these effects are not particularly straightforward. Our results for this much simplified problem suggest that the problem taking into account the acceleration effect should be an intriguing one.

ACKNOWLEDGEMENTS

The work of the authors was partially supported by the Walter P. Murphy Fellowship from Northwestern University (SL), and by grant DMD-9057626 from the National Science

Foundation (PAM). The comments, suggestions and literature references provided by the anonymous reviewers of an earlier draft of this paper are also gratefully acknowledged.

REFERENCES

Aki, K. and Richards, P. G. (1980) *Quantitative Seismology*. W. H. Freeman, New York.
Auld, B. A. (1973) *Acoustic Fields and Waves in Solids*. John Wiley & Sons, New York.
Berlincourt, D. A., Curran, D. R. and Jaffe, H. (1964) Piezoelectric and piezomagnetic materials and their function in transducers. *Physical Acoustics* (ed. W. P. Mason), Vol. I-A, pp. 169–270. Academic Press, New York.
Bleustein, J. L. (1968) A new surface wave in piezoelectric materials. *Appl. Phys. Lett.* **13,** 412–413.
Brock, L. M. (1987) Two basic problems of plane crack extension: A unified treatment. *Int. J. Engng Sci.* **15,** 527–536.
Chen, P. J. (1983) Characterization of the three dimensional properties of poled PZT 65/35 in the absence of losses. *Acta Mech.* **47,** 95–106.
Deeg, W. F. (1980) The analysis of dislocation, crack and inclusion problems in piezoelectric solids. PhD thesis, Stanford University.
Freund, L. B. (1972) Crack propagation in an elastic solid subjected to general loading. I: constant rate of extension. *J. Mech. Phys. Solids* **20,** 120–140.
Freund, L. B. (1990) *Dynamic Fracture Mechanics*. Cambridge University Press, Cambridge.
Ikeda, T. (1990) *Fundamentals of Piezoelectricity*. Oxford University Press, Oxford.
Jackson, J. D. (1974) *Classical Electrodynamics*. John Wiley & Sons, New York.
Li, S. and Mataga, P. A. (1996) Dynamic crack propagation in piezoelectric materials—part I. Electrode solution. *J. Mech. Phys. Solids* **44,** 1799–1830.
Maugin, G. A. (1994) On the J-integral and energy-release rate in dynamical fracture. *Acta Mech.* **105,** 33–47.
Maugin, G. A. and Epstein, M. (1991). The electroelastic energy-momentum tensor. *Proc. Royal Soc. London, Series A* **433,** 299–312.
McMeeking, R. M. (1989) Electrostrictive stress near crack-like flaws. *Zeitschrift für Angewandte Mathematik und Physik* **40,** 615–627.
McMeeking, R. M. (1990) A J-integral for the analysis of electrically induced mechanical stress at cracks in elastic dielectrics. *Int. J. Engng Sci.* **28,** 605–613.
Pak, Y. E. (1990) Crack extension force in a piezoelectric material. *J. Appl. Mech.* **57,** 647–653.
Pak, Y. E. (1992) Linear electro-elastic fracture mechanics of piezoelectric materials. *Int. J. Fracture* **54,** 79–100.
Pak, Y. E. and Herrmann, G. (1986) Conservation laws and the material momentum tensor for the elastic dielectric. *Int. J. Engng Sci.* **24,** 1365–1374.
Pak, Y. E. and Herrmann, G. (1986) Crack extension force in elastic dielectrics. *Int. J. Engng Sci.* **24,** 1375–1388.
Parton, V. Z. and Kudryatvsev, B. A. (1988) *Electromagnetoelasticity*. Gordon and Breach, New York.
Sih, G. C. and Chen, E. P. (1977) Cracks moving at constant velocity and acceleration. *Mechanics of Fracture* 4: *Elastodynamic Crack Problems* (ed. G. C. Sih), chapter 2, pp. 59–117. Noordhoff, Amsterdam.
Suo, Z., Kuo, C.-M. Barnett, D. M. and Willis, J. R. (1992) Fracture mechanics for piezoelectric ceramics. *J. Mech. Phys. Solids* **40,** 739–765.
Vukobrat, M. (1994) On the J-integral and energy release rate in an elastic dielectric. *Int. J. Engng Sci.* **32,** 1151–1155.
Yoffe, E. H. (1951) The moving Griffith crack. *Phil. Mag.* **42,** 739–750.
Zhang, T.-Y. and Hack, J. E. (1992) Mode-III crack in piezoelectric materials. *J. Appl. Phys.* **71,** 5865–5870.